JOURNAL OF GEOPHYSICAL RESEARCH, VOL. 104, NO. D11, PAGES 13,749–13,769, JUNE 20, 1999

A study of sulfur dioxide oxidation pathways over a range of liquid water contents, pH values, and temperatures

Jinyou Liang and Mark Z. Jacobson

Department of Civil and Environmental Engineering, Stanford University, Stanford, California

Abstract. We examine factors controlling the photochemical oxidation of SO_2 in tropospheric aerosols using a gas-aqueous photochemical model. Over a range of liquid water contents (3×10^{-4} g H_2O m^{-3} to 9 g H_2O m^{-3}) and pH values (0 to 8), we find that H_2O_2(aq) and O_3(aq) provide the major sinks for SO_2 in the aqueous phase when pH is held constant at below 5 and larger than 6, respectively. OH(aq) may be an important oxidant of SO_2 in the aqueous phase when pH is held constant between 5 and 6 and H_2O_2 is depleted in an air parcel. When pH is allowed to vary during the integration, H_2O_2(aq) is the most important oxidant in the aqueous phase. O_3(aq) is important primarily when the liquid water content is large (> 1 g m^{-3}) and the solution pH is above 4. O_3(aq) is also important when the pH is initially high (> 6) for quickly oxidizing SO_2 and, thereby, reducing the pH into the pH region where H_2O_2(aq) is the most important oxidant. OH(aq) may be important when H_2O_2 is depleted and the liquid water content is large. When aerosols are present during noncloudy days in summer, the aqueous-phase oxidation of SO_2 is insignificant compared with the gas-phase oxidation of SO_2. We find, however, that the SO_2 oxidation in wet aerosols may be enhanced in winter or when the temperature is low (273 K) and the relative humidity is high. Uncertainties in the reaction rate coefficients may significantly affect the concentrations of oxidants and other compounds of photochemical origin. Using a relatively stringent criterion, a compressed gas-aqueous phase chemical mechanism for photochemical oxidation of SO_2 is proposed for global tropospheric modeling.

1. Introduction

Atmospheric sulfate is environmentally important. It is a component of acid rain, which is harmful to crops, plants, and freshwater reservoirs. It is also a component of tropospheric aerosols, which affect Earth's radiation budget. In the stratosphere, sulfate aerosols often serve as nuclei for polar stratospheric cloud particles.

Oxidation of sulfur dioxide is the most important anthropogenic source of sulfate in the free troposphere. This oxidation is relatively slow in the gas phase (~1 day lifetime), but more rapid in the aqueous phase. The speed of aqueous oxidation depends on pH, liquid water content, and the availability of oxidants [*Pandis and Seinfeld*, 1989; *Gurciullo and Pandis*, 1997]. In a cloud, oxidation of sulfur dioxide occurs predominantly in the aqueous phase [*Chameides and Davis*, 1982; *Wang and Chang*, 1993] owing to the presence of a sufficiently high liquid water content. The contribution of aqueous-phase formation of sulfate in clouds to the total sulfate production in the troposphere is, however, limited by the relatively small total volume of cloud water in the troposphere [*Liang and Jacob*, 1997]. Unlike clouds, aerosols are ubiquitous in the troposphere. The liquid water content of an aerosol plume, even in polluted air, is about 1000 times smaller than that of a cloud. As a result, processing of sulfur dioxide in aerosols is much slower than that in clouds [*Jacobson*, 1997a,b]. However, because aerosols are ubiquitous in the free troposphere, they may contribute to significant aqueous-phase formation of sulfate on a global scale.

Computational limitations have inhibited global tropospheric models from including large numbers of chemical reactions. Of the thousands of chemical reactions available to describe photochemistry in the troposphere, a small portion of them may account for much of the photochemical oxidation of SO_2 in the free troposphere. Meanwhile, uncertainties in reaction rate coefficients inevitably propagate to the calculation of photochemical oxidation of SO_2. It is therefore useful to provide a compressed reaction mechanism for simulating the photochemical oxidation of SO_2 on a global scale, providing that the resulting error is insignificant compared with that propagated from uncertainties in reaction rate coefficients.

In this paper, we first examine factors controlling the photochemical oxidation of SO_2 in tropospheric aerosols over a range of pH values and liquid water contents. Then we evaluate sensitivities of sulfate production to uncertainties in reaction rate coefficients. Finally, we construct a compressed chemical mechanism for the oxidation of SO_2, using a gas-aqueous photochemical model.

2. Model and Simulations

We use a gas-aqueous photochemical box model to simulate the chemical transformation of an air parcel. We summarize the chemistry and numerical methods used in the model below.

Paper number 1999JD900097.
0148-0227/99/1999JD900097$09.00

2.1. Chemical Environment

We include a CH_4-C_2H_6-CO-NO_x-SO_2 gas-phase photochemical mechanism in our calculations. Gas-phase reaction rate coefficients are taken from *Atkinson et al.* [1997], who provide evaluated mean coefficients and their standard deviations. Mass fluxes of SO_2, O_3, OH, HO_2, H_2O_2, CH_3O_2, CH_3OOH, and HCOOH between the gas phase and wet aerosols are calculated following the method described by *Jacob* [1986] by assuming an accommodation coefficient of 0.1. A change in the reaction probability of severalfold results in only a small difference (< 20%) in the concentrations of important aqueous species [*Jacob*, 1986]. Aerosols and cloud droplets are assumed to be monodisperse and of uniform composition. We treat concentrations of HCHO and HNO_2 in the gas phase to be in equilibrium with that in the aqueous phase.

Aqueous-phase kinetic reactions are taken from the published literature, and some of those references contain more primary sources. We include recent kinetic data for reactions involving Cl(aq), NO_3(aq), and SO_4^- radicals [*Exner et al.*, 1992, 1994; *Chin and Wine*, 1994; *Bao and Barker*, 1996; *Jacobi et al.*, 1997]. A series of papers using these reactions have been published in the last decade [e.g., *Chameides and Davis*, 1982; *Jacob*, 1986; *Lelieveld and Crutzen*, 1990; *Liang and Jacob*, 1997]. A goal of this study is to demonstrate a quantitative method for constructing a compressed gas-aqueous reaction mechanism from a larger mechanism after considering that some of the reactions account for much of the total production and loss of important species in the system. We do not evaluate the original aqueous-phase kinetic reactions. Instead, we cite their original sources and comment on their uncertainties. Thus our conclusions inherit all the possible errors embedded in the original kinetic data, like in all previous modeling studies. We do not include aqueous-phase reactions involving trace-metal ions in this study, since few data are available for concentration levels of those ions in the aqueous phase of aerosols and clouds in much of the troposphere.

2.2. Ionic Activity Coefficients

An outstanding issue in this study is the calculation of ionic activity coefficients at low pH and liquid water content when the ionic strength (denoted as I) is relatively high. The ionic strength is defined as $0.5\sum_i m_i z_i^2$, where m_i and z_i are the molality (mole per kilogram of water, or m hereafter) and the charge number of ion i, respectively. At relatively low ionic strength (I < 0.1 m) when the *Davies* [1938] equation is applicable, we explicitly calculate the concentration constants of equilibrium and gas-aqueous flux reactions from corresponding activity constants by using relevant activity coefficients of involved ions. The activity coefficient (γ) of ion i is calculated with

$$-\log_{10}\gamma_i = A\, z_i^2\left\{\frac{\sqrt{I}}{1+\sqrt{I}} - b\, I\right\} \quad (1)$$

where z_i denotes the charge of ion i, $A = 0.509\,(T/298.15)^{1.5}$, and b is an empirical parameter with the value chosen to be 0.3 here [*Davies*, 1938]. For kinetic reactions involving ions, we apply the Debye-Huckel-Bronsted-Davies equation [*Bao and Barker*, 1996] to correct for ionic effects on both reactants and transition-state intermediates:

$$\log k = \log k^0 + 2\, z_1\, z_2\, A\left\{\frac{\sqrt{I}}{1+\sqrt{I}} - b\, I\right\} \quad (2)$$

where k denotes kinetic rate constant at ionic strength I, and k^0 at infinitely dilute aqueous solution. z_1 and z_2 denote the charges of aqueous reactants 1 and 2, respectively. A and b are the same as in equation (1). We choose a conservative upper bound for I in equations (1)-(2) due to the following considerations. Equation (2) contains the transition-state theory for kinetic reactions and the assumption that the reaction rate is proportional to the concentration rather than the activity of the activated intermediate, in its derivation. It is shown that equation (2) operates well at I < 0.1 m for a number of solutions [*Finlayson-Pitts and Pitts*, 1986, pp. 279-280]. But, at higher ionic strength for some solutions, another theory, such as ion-pair theory, must be invoked on top of equation (2) in order to explain the experimental data [*Bao and Barker*, 1996].

At relatively high ionic strength (6 m ≥ I ≥ 0.1 m), such as when the liquid water content and/or pH is low, we calculate mean mixed activity coefficients for ion pairs in equilibrium reactions using *Bromley*'s [1973] method as described by *Jacobson et al.* [1996] and *Jacobson* [1999]. We present the formulation for calculating mean mixed activity coefficients in Appendix A. For kinetic and gas-aqueous flux reactions involving ions, we estimate activity coefficients of individual ions using *Pitzer*'s [1991] equations with necessary parameters taken from *Rosenblatt* [1981] and *Pitzer* [1991]. Because of the dearth of parameters and their expected insignificance, the interactions between ions with like charges were omitted in the calculation. The formulas for calculating ionic activity coefficients using Pitzer's equations are shown in Appendix B. Activity coefficients of formic- and acetic-acid ions are calculated following *Partanen* [1996], which is valid for ionic strengths up to 2 m. When the ionic strength is larger than 2 m at liquid water content of 3×10^{-4} g m^{-3}, we use the values at the upper limit of the valid range for formic- and acetic-acid ions. Assumptions have to be made for ions and ion pairs without relevant measurements. Ions present in significant concentrations in our model include H^+, NH_4^+, SO_4^{2-}, HSO_4^-, HSO_3^-, SO_3^{2-}, and NO_3^-. Following the method described by *Rosenblatt* [1981], we assumed that the activity coefficient of NO_2^- is that of NO_3^-, and O_2^- is that of Cl^-. Activity coefficients of HSO_3^-, $HOCH_2SO_3^-$, HSO_5^-, SO_5^-, and SO_4^- were assumed to be that of HSO_4^-, and that of SO_3^{2-} was assumed to be that of SO_4^{2-}. We conducted sensitivity tests to check the effect of a factor of 2 difference in the estimated activity coefficients for the minor ions and discuss the results in section 3. The upper limit of ionic strength (6 m) in the model is chosen so that Pitzer's theory is applicable.

The concentration of relatively inert electrolytes in aerosols available for incorporation into the aqueous phase may vary considerably, depending on the sources of aerosols. In the free troposphere, however, NH_4^+, NO_3^-, and SO_4^{2-} are important components of aerosols [*Liang et al.*, 1998]. We assume a uniform concentration, for the total concentration of inert electrolytes in aerosols, equivalent to about 1×10^{-5} g m^{-3} NH_4NO_3 on the basis of contribution to ionic strength. Charge balance is maintained in the model by varying the concentration of ammonium or nitrate. The contribution of inert electrolytes in aerosols to ionic strength is significant when liquid water content is small. For example, when the liquid water content is 3×10^{-4} g m^{-3}, the ionic strength contributed from inert electrolytes is about 0.3 m.

2.3. Photolysis Coefficients

We calculate photolysis coefficients over the UV and visible radiation spectra using a six-stream radiative-transfer model

described by *Logan et al.* [1981], with overall line resolution of ~5 nm, and ~0.26 nm for the Shumann-Runge band. For the calculation of radiative transfer, we separate the atmosphere into 55 vertical layers with ~1 km resolution in the troposphere and ~2 km above the tropopause. We use climatological vertical profiles of O_3 and temperature as in previous studies. A light-absorbing aerosol is included with an optical depth of 0.1 at 310 nm varying inversely with wavelength [*Liang et al.*, 1998].

2.4. Numerical Method

We solve gas and aqueous chemistry with a Newton-Raphson iterative method that uses sparse-matrix techniques. In order to include sparse-matrix techniques, we translate the original formula [e.g., *Press et al.*, 1992] into equation (3) for solving concentrations at the end of a time step (Δt):

$$C_{n+1} - C_n = \frac{\Delta t\,(R_p - R_l) + C_0 - C_n}{I - \Delta t\, J} \tag{3a}$$

$$J = \frac{\partial (R_p - R_l)}{\partial C} \tag{3b}$$

where C and R denote vectors of concentrations and corresponding reaction rates, respectively. I denotes a unit matrix. The subscripts 0, n, and n+1 denote the beginning of a time step, the n-th iteration and the (n+1)-th iteration, respectively. The subscripts p and l denote production and loss, respectively. Equation (3) preserves the superconvergence of the Newton-Raphson method [e.g., *Press et al.*, 1992].

To allow for aqueous dissociation and phase equilibrium, we calculate the Jacobian (3b) analytically and solve simultaneous differential equations of independent variables (Table 1) resulting from (3). For those species involved in an aqueous dissociation or phase equilibrium, we define a new independent variable in (3) and exclude those species (hereafter termed family members of the new independent variable) from (3). We give an example below to illustrate how to complete an iteration for the new independent variable dealing with gas-aqueous phase equilibrium. The concentration of the new independent variable C_T is defined as the sum of the gas-phase concentration (C_g) and the aqueous-phase concentration (C_a) of species C:

$$C_T = C_g + C_a \tag{4a}$$

When C_g and C_a are at equilibrium, we have

$$C_a = k_C\, C_g \tag{4b}$$

$$C_g = k_g\, C_T \tag{4c}$$

$$C_a = k_a\, C_T \tag{4d}$$

The R_p and R_l in (3) for C_T is calculated by summing up the R_p and R_l for C_g and C_a, respectively. The Jacobian for C_T is calculated by substituting C_g and C_a with C_T in relevant terms using (4c) and (4d), respectively. Hence C_T is calculated directly from (3) at each iteration. We then extract C_g and C_a by using (4c) and (4d). The same procedure is applicable also to aqueous dissociation.

2.5. Simulations

We list in Table 2 the simulations conducted for this study and their initial conditions. The purpose of the simulations was to estimate the effects of liquid water content, pH, temperature, and radiation on sulfate production in the gas and aqueous phases. For each type of simulation, the concentrations of NO_x (NO + NO_2), CO, CH_4, and C_2H_6 were held constant throughout the calculations, but the initial concentration of SO_2 was set to 10 ppbv for the high-SO_2 case and 100 pptv for the low-SO_2 case. For each case, we conducted two runs, one with a variable and one with a constant pH. The constant pH cases were obtained by applying a changing source of ammonium to the aqueous phase. The variable pH cases were obtained by integrating the chemistry without applying additional ammonium to the aqueous phase. Without the alkaline (ammonium) source, the solution pH decreases during the oxidation of SO_2, and the variable pH is obtained. The calculations started with initial conditions at 1000 hours and proceeded to 1700 with fixed time steps of 90 s for the first half hour and of 15 min for the rest of the integration period.

Table 1. Species Defining Chemical Environment

Group	Species
Sulfur compounds	
	1. SO_2=SO_2(g)
	2. S(IV)=SO_2(aq) + HSO_3^- + SO_3^{2-}
	3. $HOCH_2OSO(OH)$(aq)
	4 HSO_5^-
	5. SO_5^-
	6. SO_4^-
	7. $SO_{4,T}^{2-}$=H_2SO_4(g) + H_2SO_4(aq) + HSO_4^- + SO_4^{2-}
Oxidants	
	8. O_3=O_3(g)
	9 O=O(g)
	10. $O(^1D)$=$O(^1D)$(g)
	11. OH=OH(g)
	12. HO_2=HO_2(g)
	13. H=H(g)
	14. H_2O_2=H_2O_2(g)
	15. O_3(aq)
	16. OH(aq)
	17. H_2O_2(aq)
	18. HO_2(aq,T)=HO_2(aq) + O_2^-
Nitrogen compounds	
	19. $NO_{2,T}$=NO_2(g) + NO_2(aq)
	20. NO_T=NO(g) + NO(aq)
	21. $HNO_{2,T}$=HNO_2(g) + HNO_2(aq)
	22. HNO_4=HNO_4(g)
	23. NO_3=NO_3(g)
	24. N_2O_5=N_2O_5(g)
	25. NH_3=NH_3(g)
	26. HNO_3=HNO_3(g)
	27. NH_4^+
	28 NO_3^-
Organic species	
	29. CH_4=CH_4(g)
	30. C_2H_6=C_2H_6(g)
	31. $HCHO_T$=HCHO(g) + HCHO(aq) + $H_2C(OH)_2$(aq)
	32. CH_3CHO=CH_3CHO(g)
	33. CH_3O_2=CH_3O_2(g)
	34. CH_3O_2(aq)
	35. $C_2H_5O_2$=$C_2H_5O_2$(g)
	36. CH_3OOH=CH_3OOH(g)
	37. CH_3OOH(aq)
	38. C_2H_5OOH=C_2H_5OOH(g)
	39. $HCOOH_T$(aq)=HCOOH(aq) + $HCOO^-$
	40. HCOOH=HCOOH(g)
	41. CH_3COOH_T=CH_3COOH(g) + CH_3COOH(aq) + CH_3COO^-(aq)
	42. C_2H_5OH=C_2H_5OH(g)
	43 CH_3OH_T=CH_3OH(g) + CH_3OH(aq)
	44. CH_3CO_3=CH_3CO_3(g)
	45. $CH_3C(O)OOH_T$=$CH_3C(O)OOH$(g) + $CH_3C(O)OOH$(aq)
	46. PAN=$CH_3C(O)O_2NO_2$(g)

Table 2. Simulations and Their Initial Conditions

Parameter	Baseline Simulation	Low-Temperature Simulation	High-HCHO Simulation	Winter Simulation	Low-H_2O_2 Simulation	Compressed Simulation
1. NO_x, pptv	40	40	4000	1000	40	40
2. CO, ppbv	85	85	400	150	85	85
3. O_3, ppbv	30	30	100	30	30	30
4. HCHO, ppbv	1	1	10	1	1	1
5. CH_3CHO, pptv	100	100	1000	100	100	100
6. PAN, pptv	100	100	1000	100	100	100
7. H_2O_2, ppbv	1	1	1	1	0.05	1
8. Temperature, K	298	273	298	273	298	298
9. Latitude, °N	0	0	0	40	0	0
10. Solar declination, deg	0	0	0	-15	0	0
11. Column O_3, DU	250	250	250	350	250	250
12. Altitude, km	1.5	1.5	1.5	1.5	1.5	1.5
13. Actinic flux, W m^{-2}	389	389	389	269	389	389

The initial concentration of SO_2 was 10 ppbv for the high-SO_2 case and 100 pptv for the low-SO_2 case. Here 1 DU = 2.687×10^{16} molecules cm^{-2}. NO_x concentration was fixed at the initial condition throughout the simulations. Concentrations of CH_4 and C_2H_6 were held constant at 1.7 ppmv and 1.1 ppbv, respectively. Relative humidity was fixed at 100% for all simulations. Species not listed above were initialized with negligible concentrations. Actinic fluxes are listed at 1.5 km at noon.

The integration method was iterative and implicit. Actinic fluxes were calculated at each time step. The baseline simulation was used for all discussions below unless otherwise indicated.

To show the effects of uncertain chemical rate coefficients on concentration uncertainties, we ran 1000 simulations with chemical rate coefficients sampled randomly, using a subtractive method [*Press et al.*, 1992], to be the mean plus or minus one standard deviation. As a result, our estimated uncertainty from errors in chemical rate coefficients should be understood as the maximum pertinent to one standard deviation recommended. The means and standard deviations of chemical kinetic rate coefficients were taken from *Atkinson et al.* [1997] for gas-phase reactions. The standard deviations may slightly vary with temperature for some reactions in the original recommendation. We used the standard deviations at 298 K, and this simplification should not alter our conclusions below. We applied a 10% coefficient of variation, defined as the standard deviation divided by the mean, for all photolysis rate coefficients, though the actual error may be smaller for some well-studied species such as ozone (R. Salawitch, personal communication, 1998). Considering that the uncertainty in actinic flux calculation, especially due to clouds in the lower troposphere, may be up to 50-100% (C.J. Walcek, personal communication, 1998), we did a sensitivity test with a 100% coefficient of variation for all photolysis coefficients. For aqueous-phase reactions, we used a 20% coefficient of variation in the simulation, which is the uncertainty of the oxidation of S(IV) by H_2O_2(aq). A sensitivity test with a 50% coefficient of variation for aqueous-phase reactions was also conducted, since many aqueous reactions may have significantly larger uncertainties in rate coefficients. Two sensitivity tests were conducted to check the effect of a factor of 2 difference in the estimated activity coefficients for the minor ions.

3. Formation of Sulfate in Wet Aerosols

In this section, we investigate factors controlling the formation of aqueous-phase sulfate. Formation of sulfate in the aqueous phase originates from the oxidation of S(IV) by H_2O_2(aq), O_3(aq), CH_3OOH(aq), and OH(aq). All the above reactions are sensitive to pH, liquid water content, temperature, and radiation.

3.1. Sulfate Growth Curves

Figure 1 shows the amount of sulfate produced from each oxidation route of S(IV) in the aqueous plus gas phases in the high- and low-SO_2 cases of the baseline simulation when the pH varied. As shown in the left panel of Figure 1, gas-phase formation of sulfuric acid dominated at low liquid water content (H_2O = 3×10^{-4} g m^{-3}). When the liquid water content was 0.3 g m^{-3}, such as in a nonprecipitating cloud, oxidation of S(IV) by H_2O_2(aq) dominated the sulfate formation, since the final pH values were below 3 for initial pH values of 3, 5, and 7. At high liquid water content (3 g m^{-3}), when final pH values are above 4, OH(aq) became an important oxidant in the high-SO_2 case and O_3 became important in the low-SO_2 case. When H_2O_2 was depleted from its initial concentration, as in the high-SO_2 case when S(IV) was high, photochemical production of H_2O_2 in the gas phase was reduced, and photochemical loss of H_2O_2 in the aqueous phase was enhanced in clouds [*Liang and Jacob*, 1997]. In these cases, the importance of H_2O_2(aq) in the formation of sulfate was reduced. Under such conditions, OH(aq) became an important oxidant. At high pH, O_3 is an important oxidant [*Seinfeld and Pandis*, 1998]. Since the formation of sulfate reduces pH, O_3 is important only when the final pH is above 4 and when the initial pH is 7 (bottom right of Figure 1b).

3.2. Relative Importance of Aqueous-Phase Oxidants

The relative importance of primary oxidants (H_2O_2(aq), O_3(aq), OH(aq), and CH_3OOH(aq)) for the formation of aqueous-phase sulfate is shown in Figures 2-4 for the initial pH range of 0 to 8 and the liquid water content range of 3×10^{-4} g m^{-3} to 9 g m^{-3}. As shown in Figure 2 when the pH was kept constant, H_2O_2(aq) and O_3(aq) dominated sulfate production at pH < 5 and pH ≥ 6, respectively, over almost all ranges of liquid water content. At 5 ≤ pH < 6, OH(aq) may be important for the formation of sulfate when initial SO_2 is higher than H_2O_2. When initial H_2O_2 is higher than SO_2, the oxidation of S(IV) by OH(aq) is negligible except when HCHO is high and photochemistry is strong (figures not shown). The oxidation of S(IV) by CH_3OOH(aq) was insignificant in all cases.

Figure 3 shows the percentage contribution from primary oxidants to the sulfate formation in aqueous phase for the baseline

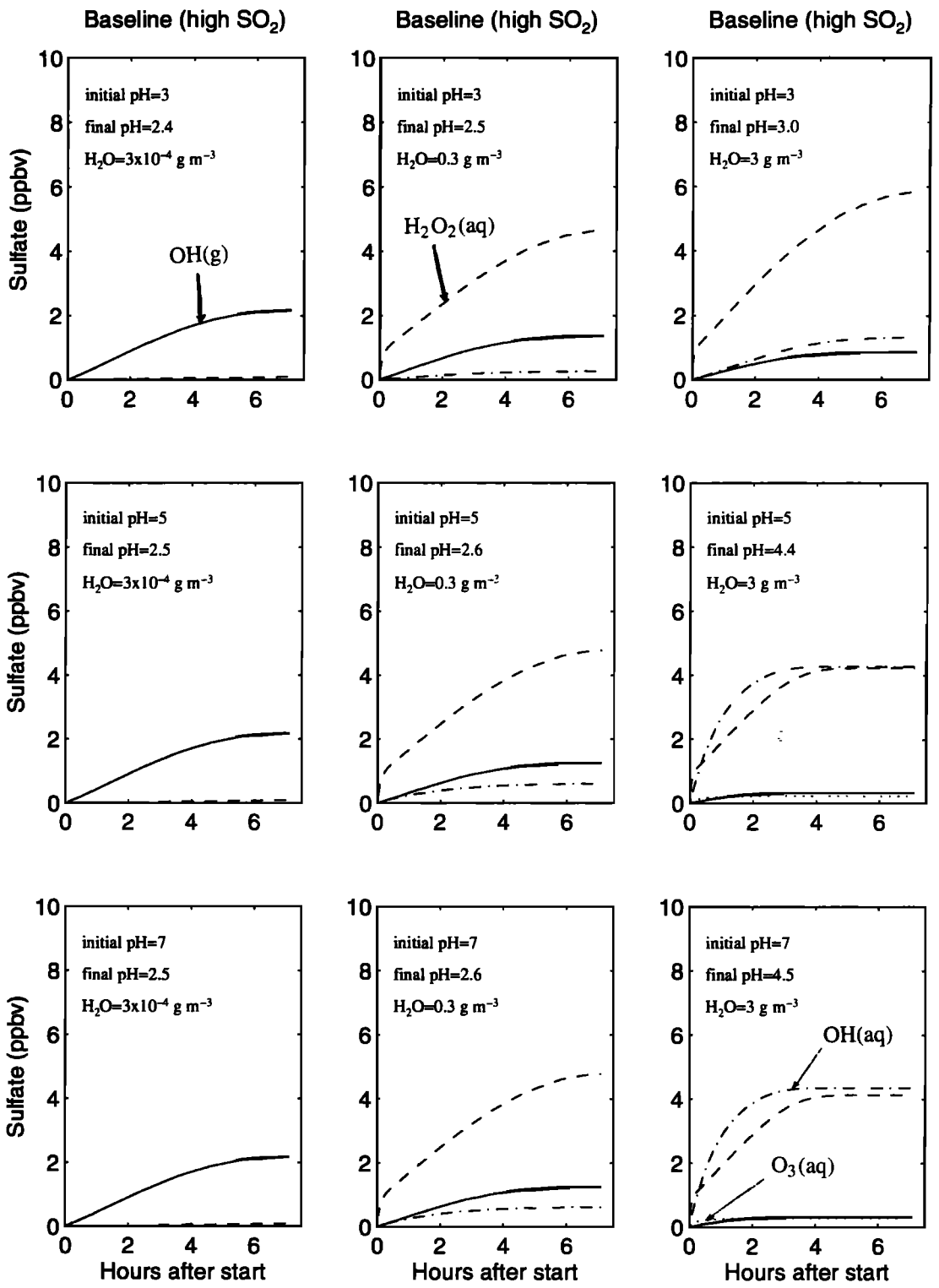

Figure 1a. Growth curves of sulfates produced from the oxidation by OH(g), H_2O_2(aq), OH(aq), and O_3(aq) in the high-SO_2 cases of the baseline simulation at a variable pH.

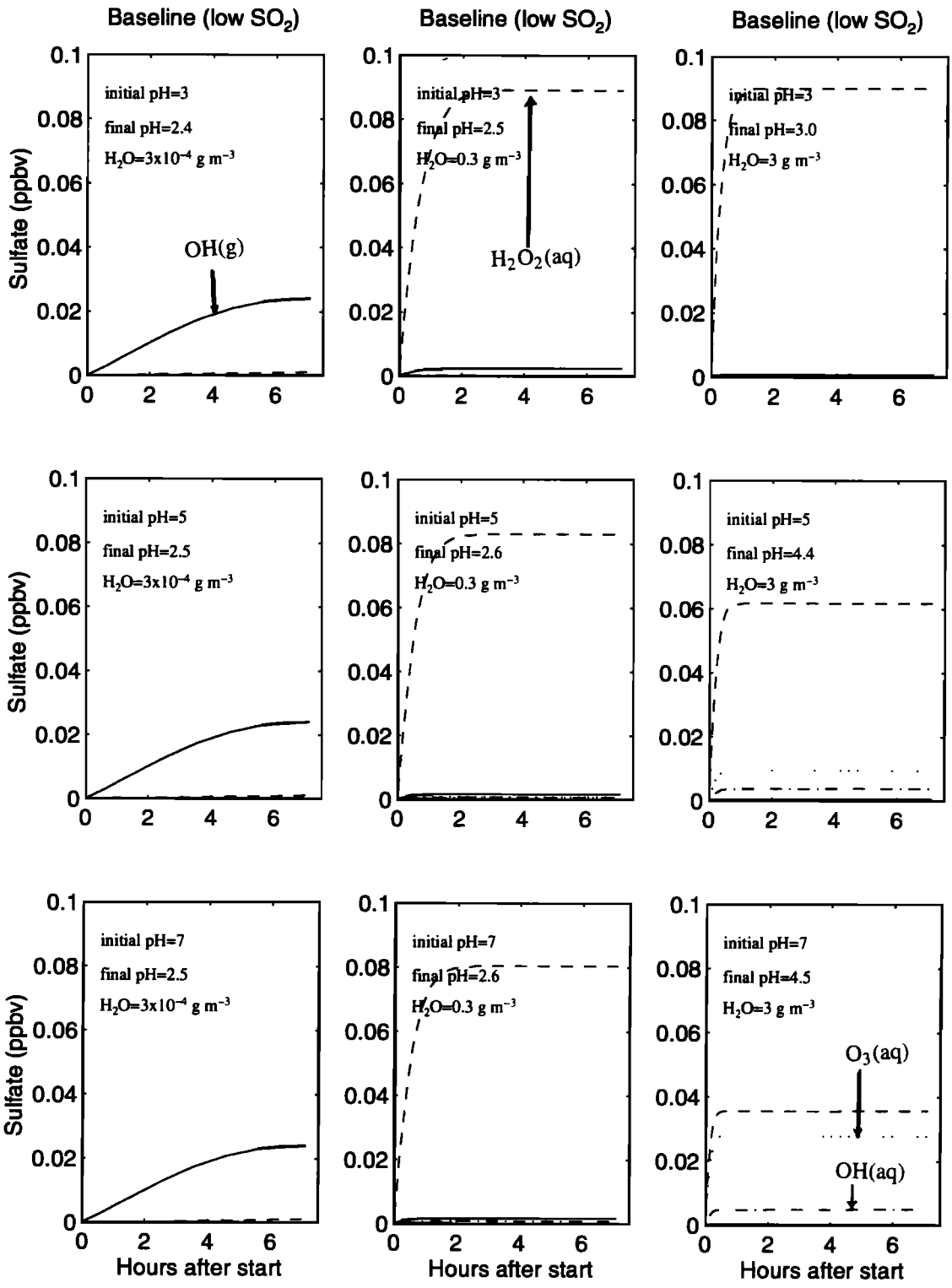

Figure 1b. Same as Figure 1a, except for the low-SO_2 cases.

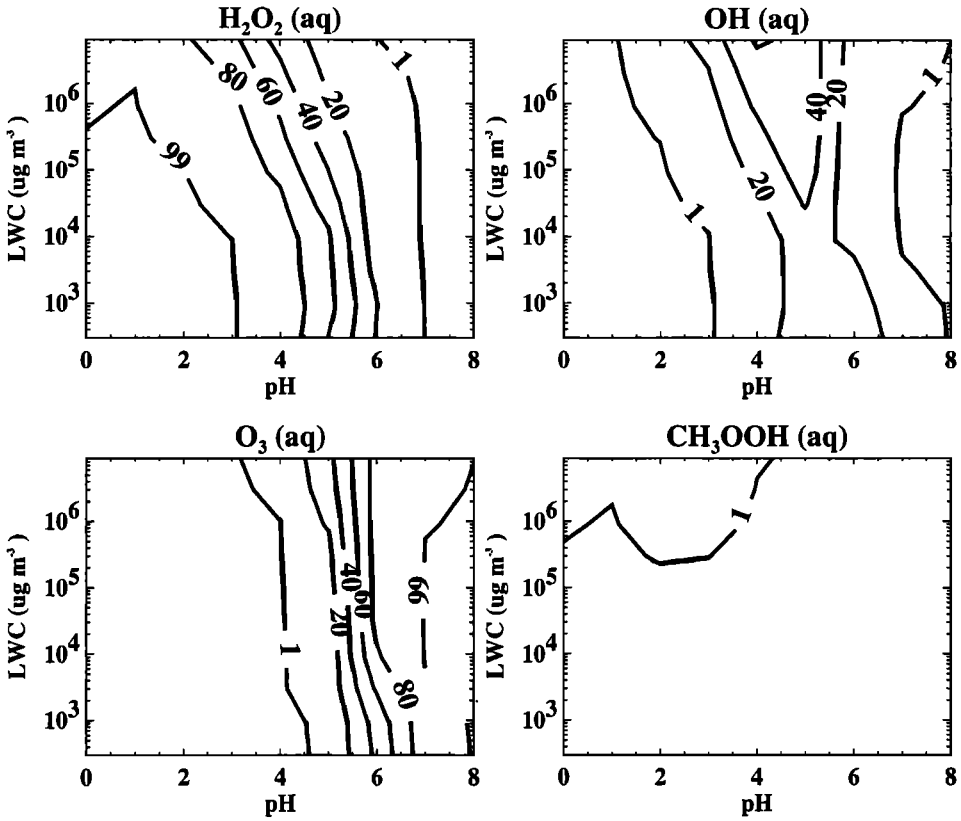

Figure 2a. Percentage contributions to the aqueous-phase sulfate production from the oxidation by H_2O_2(aq), O_3(aq), OH(aq), and CH_3OOH(aq) over the (pH-liquid water content) plane in the high-SO_2 cases of the baseline simulation at a constant pH.

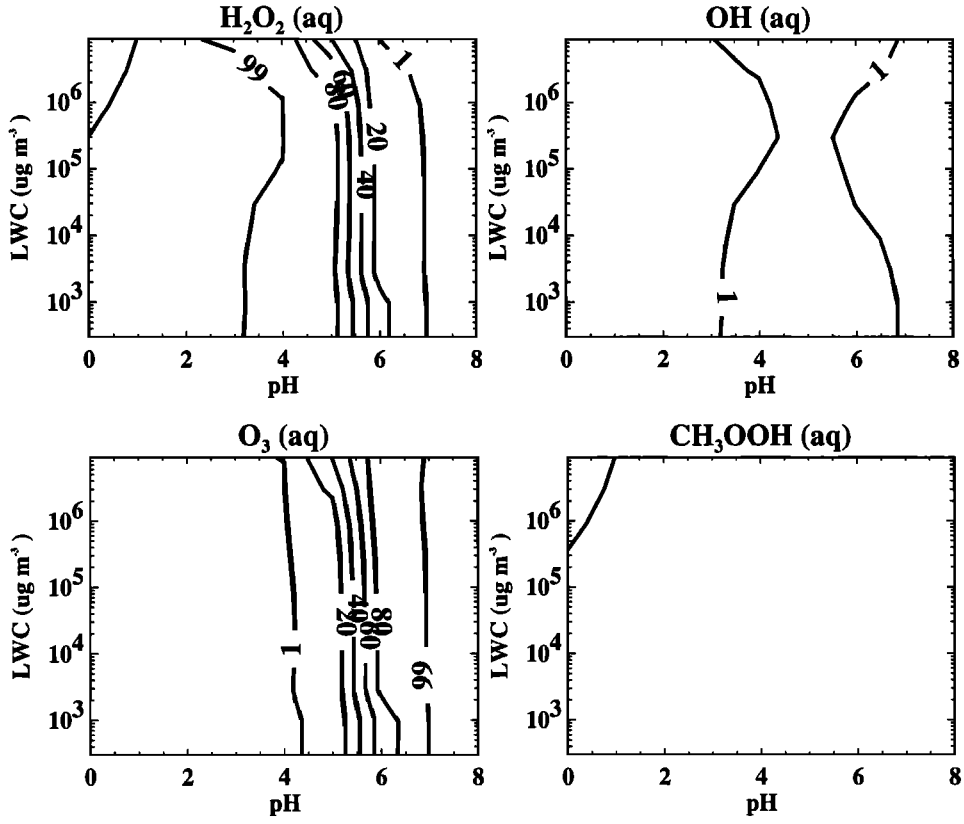

Figure 2b. Same as Figure 2a, except for the low-SO_2 cases.

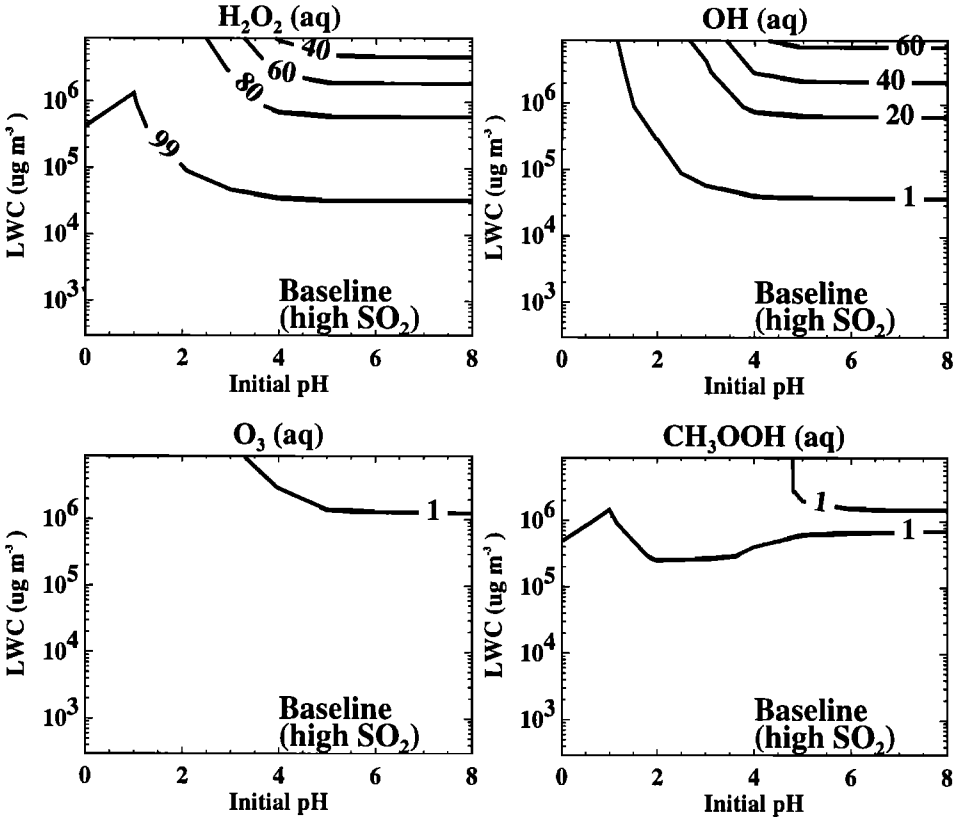

Figure 3a. Same as Figure 2a except at a variable pH.

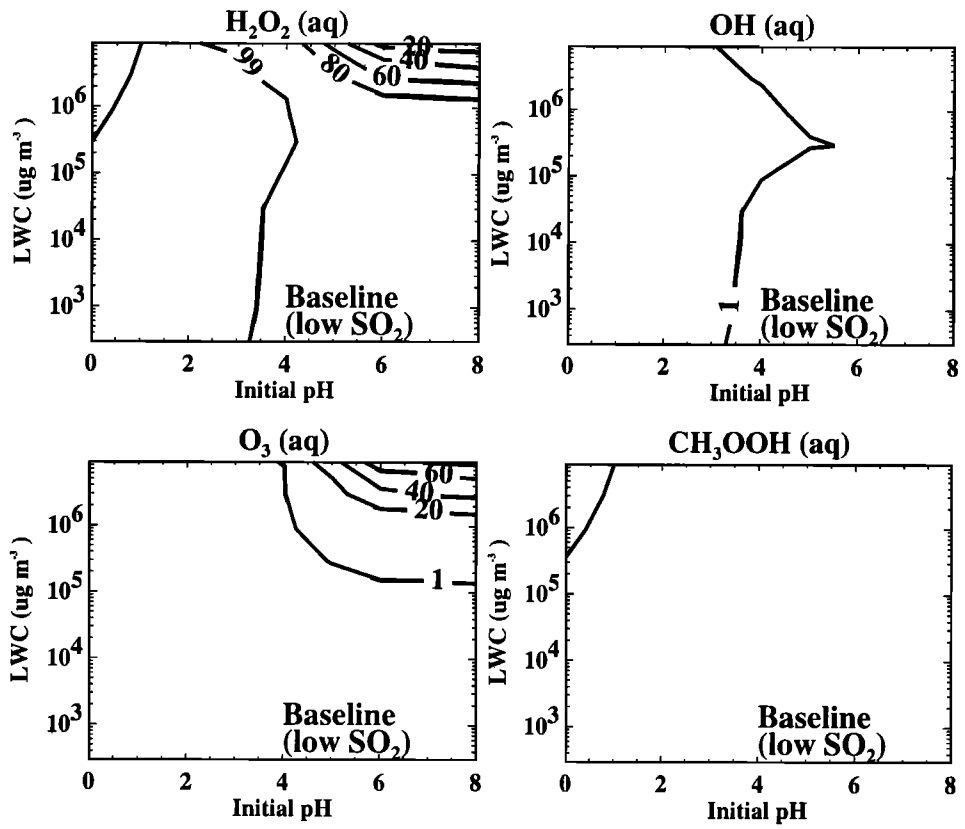

Figure 3b. Same as Figure 2b except at a variable pH.

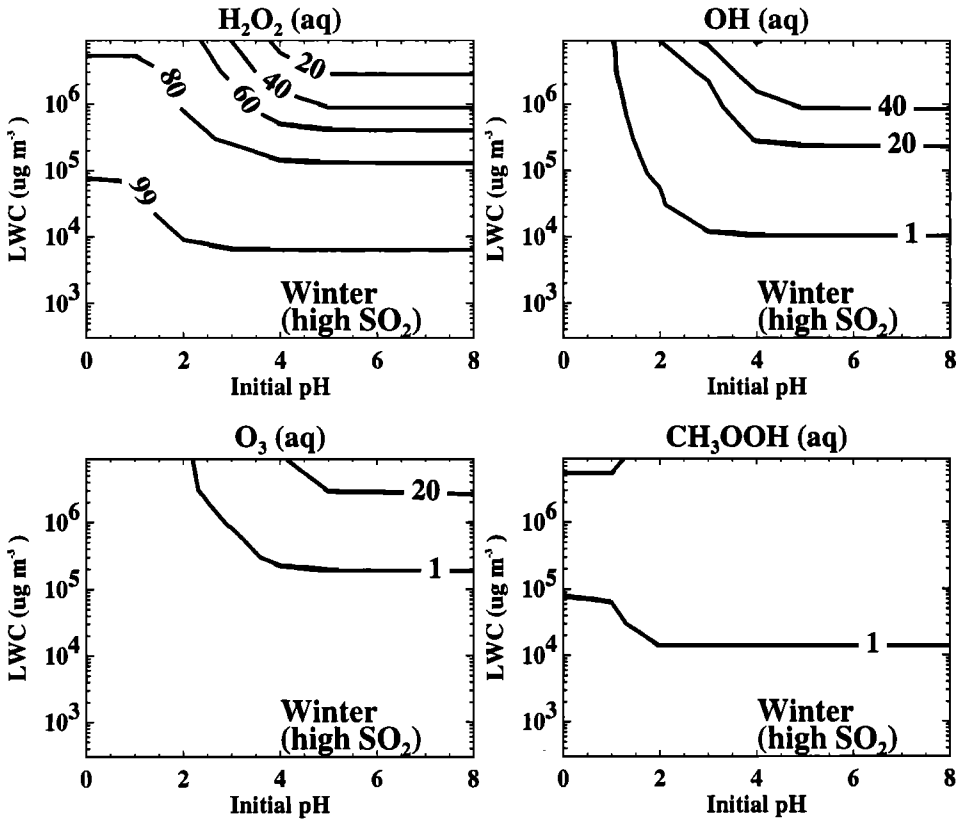

Figure 4a. Same as Figure 3a except for the winter simulation.

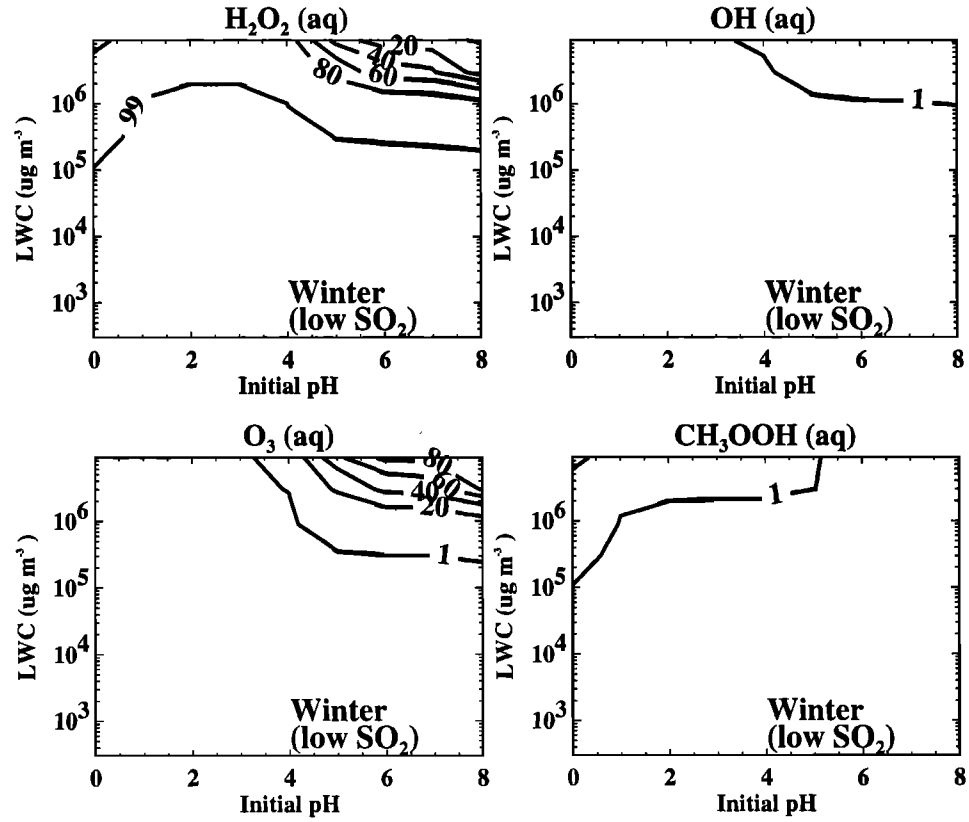

Figure 4b. Same as Figure 3b except for the winter simulation.

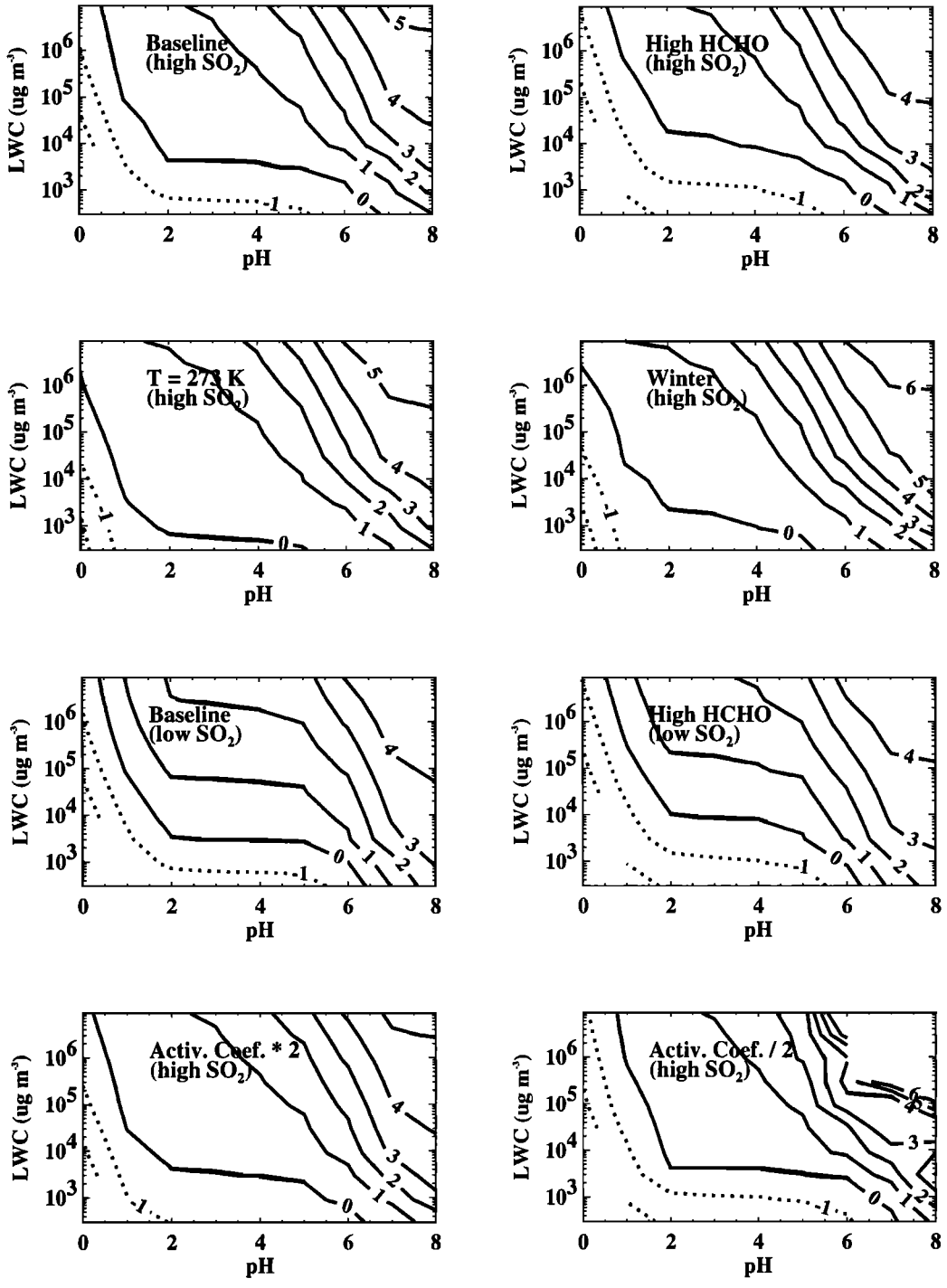

Figure 5. Ratios (in powers of 10) of the total sulfate produced in the aqueous phase to that in the gas phase over the (pH-liquid water content) plane in various simulations at a constant pH.

simulation when pH was variable. H_2O_2(aq) contributed the most in noncloudy conditions, since at relatively low liquid water content, the formation of sulfate effectively brought down the pH and inhibited the oxidation of S(IV) by O_3(aq) while gas-phase formation of H_2O_2 was still sufficient. In clouds, OH(aq) and O_3(aq) became more important in the high- and low-SO_2 cases, respectively, and H_2O_2(aq) became less important at higher liquid water content.

Figure 4 shows the same information as Figure 3 except for winter simulation. Weaker photochemistry results in less H_2O_2(aq) and OH(aq), and lower temperatures result in higher solubility of O_3. Therefore O_3(aq) becomes important at high liquid water content and high initial pH.

We ran another simulation with low initial H_2O_2 (50 pptv). The effect of low initial H_2O_2 was to enhance the importance of OH(aq) and/or O_3(aq) in the formation of sulfate by a moderate factor (results not shown).

To evaluate the relative contributions of sulfate production from gas and aqueous phases under various conditions, we show, in Figure 5, the ratio of the amount of sulfate produced in the aqueous phase to that produced in the gas phase over the pH-(liquid water content or LWC) plane for the constant pH case.

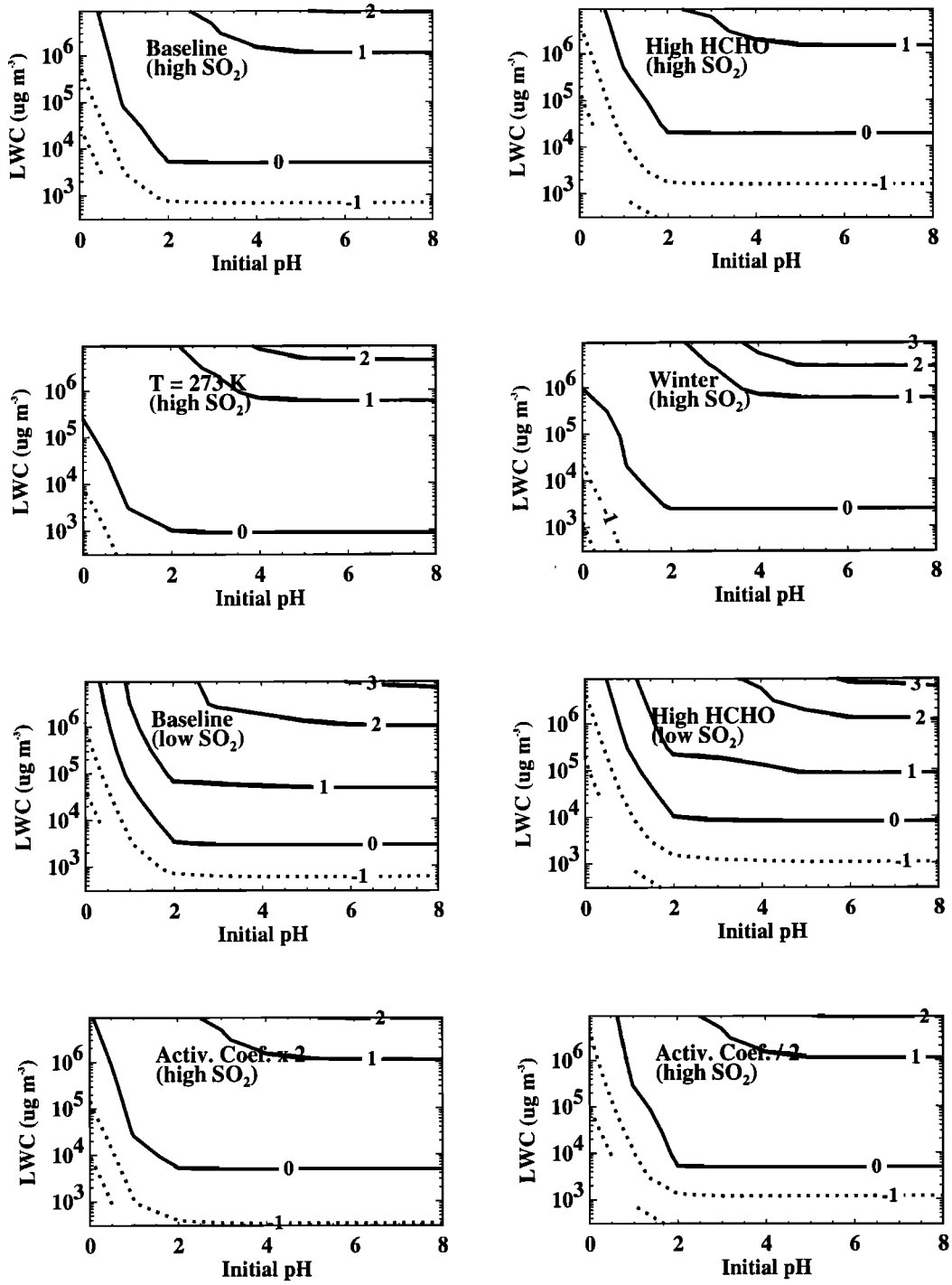

Figure 6. Same as Figure 5, except at a variable pH.

The relative importance of aqueous-phase formation of sulfate increases with pH and liquid water content in all cases. In the presence of wet aerosols over the continent or in the free troposphere over the ocean (pH < 6 and LWC < 500 μg m^{-3}), sulfate formation in the aqueous phase is smaller than that in the gas phase by a factor of up to 100. In the marine boundary layer, where the pH may be as high as 8 in sea-spray aerosols, about 100 times more sulfate is formed in the aqueous phase than in the gas phase. Sea-spray aerosols with such high pH are likely present only in the lowest few hundred meters over the ocean [*Chameides and Stelson*, 1993]. In clouds (LWC > 0.05 g m^{-3}, 2.0 < pH < 5.6), sulfate formation occurs mainly in the aqueous phase. In the presence of a fog (500 μg m^{-3} ≤ LWC ≤ 0.05 g m^{-3}), formation of sulfate is dominated by gas-phase production at low pH and LWC, and by aqueous-phase production at high pH and LWC. When the temperature is low (273 K) and the relative humidity is high or the solar radiation is weak, the relative importance of aqueous-phase oxidation of SO_2 in aerosols is enhanced.

Figure 6 shows the same information as in Figure 5 except for the variable pH case. Since the formation of sulfate reduces initial pH effectively, especially at low LWC, aqueous-phase formation of sulfate is no longer important when LWC is below a few thousand μg m^{-3} compared with the formation of sulfate in

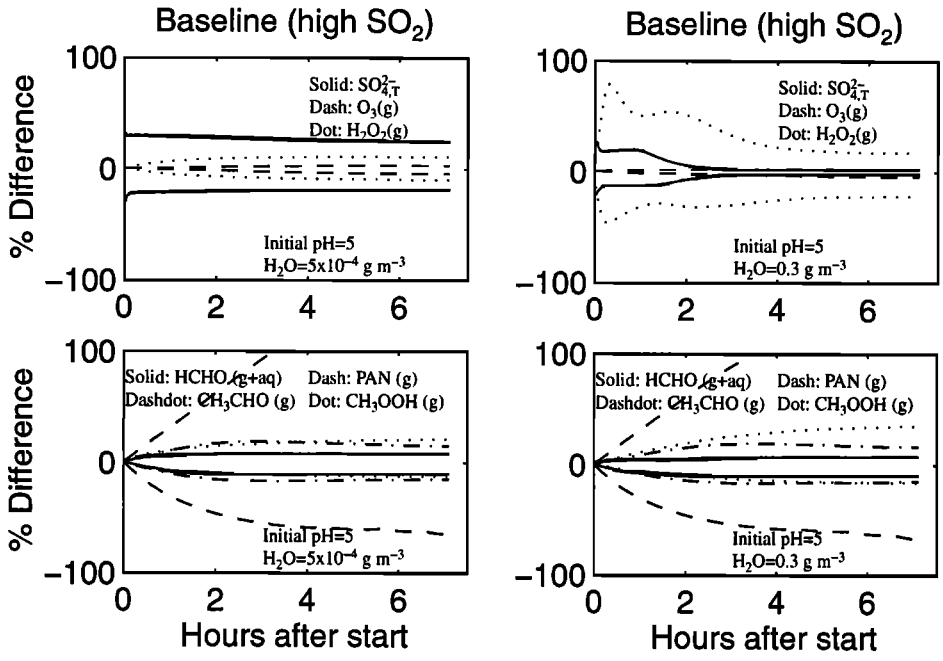

Figure 7a. Percentage difference in concentrations of sulfate, ozone, hydrogen peroxide, formaldehyde, acetaldehyde, peroxyacetylnitrate, and methylperoxide between the baseline simulation and the "1000 simulations" for the high-SO_2 cases at liquid water content of 500 μg m^{-3} (left panel, noncloudy) and 0.3 g m^{-3} (right panel, cloudy), respectively.

the gas phase. The ratio of the aqueous-phase to gas-phase formation of sulfate is reduced in cloudy conditions at high initial pH owing to the self-inhibition of the oxidation of S(IV) by O_3(aq) [*Seinfeld and Pandis*, 1998].

4. Effects of Uncertainties in Chemical Rate Coefficients on Concentrations

Figure 7 shows the percentage difference in concentrations of a list of species between the "1000 simulations", in which sampled rate coefficients were used, and the baseline simulation, in which mean rate coefficients were used at noncloudy and cloudy cases. In the noncloudy case (left panel), the relative concentration uncertainty (defined as the mean +/- 1 standard deviation in the 1000 simulations divided by the concentration in the baseline simulation and subtracted by 1) attributed to chemical rate coefficients was small for ozone (partly due to its long lifetime relative to the integration time) and hydrogen peroxide (<10%); moderate for sulfate, formaldehyde, methylperoxide, and acetaldehyde (~20%); and large for peroxyacetylnitrate (PAN) (up to 100%). In the cloudy case (right panel), the relative concentration uncertainty diminished for sulfate (0-10%) and increased for

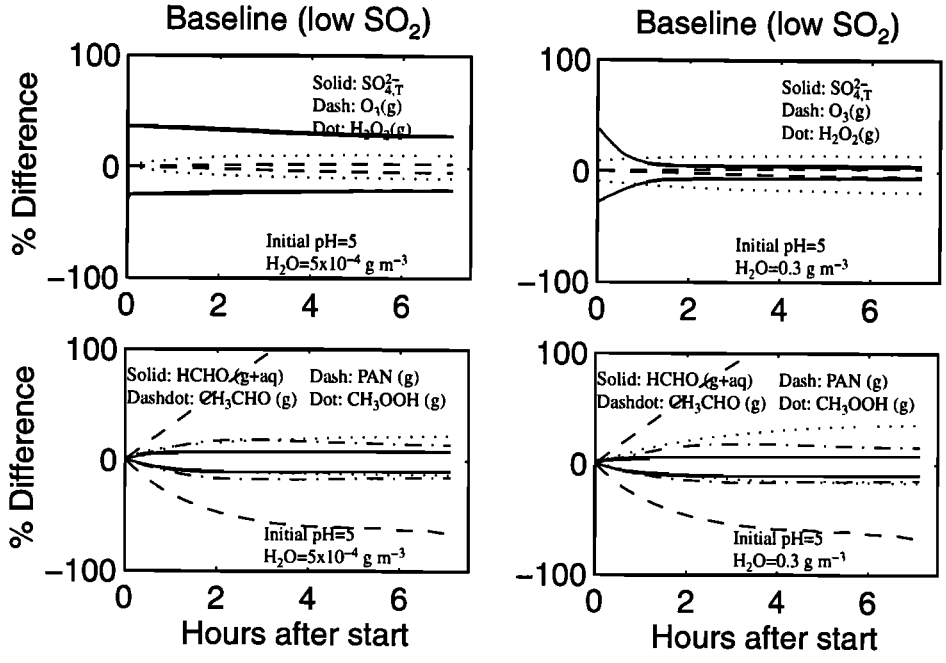

Figure 7b. Same as Figure 7a, except for the low-SO_2 cases.

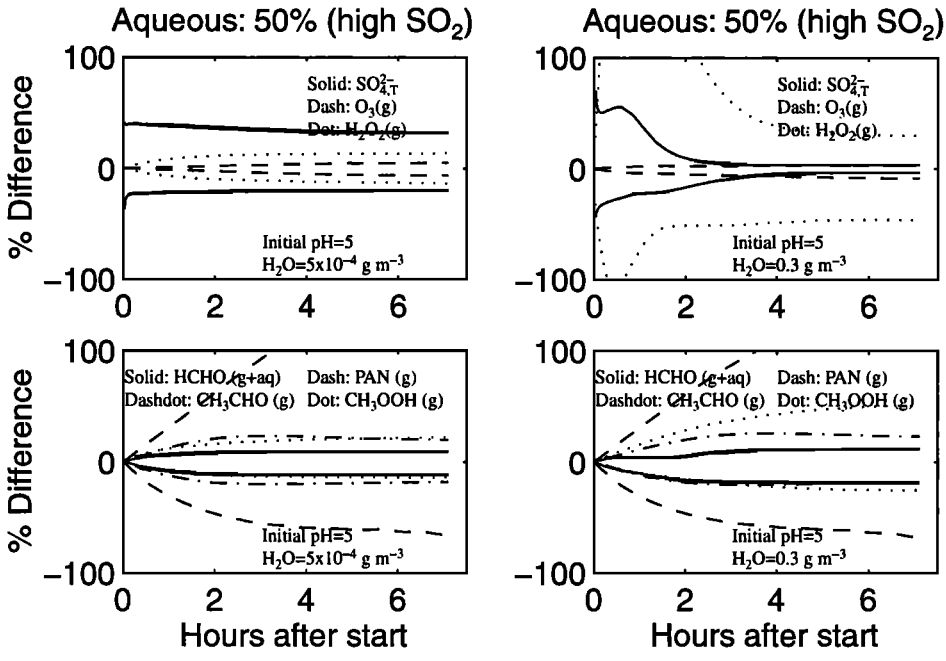

Figure 8a. Same as Figure 7a, except that the uncertainty of aqueous-phase reaction rate coefficients are assumed to be 50%, instead of 20% in Figure 7a.

hydrogen peroxide. This increase is particularly large (20-80%) in the high-SO_2 case when the initial SO_2 is higher than initial H_2O_2 (Figure 7a).

We conducted a sensitivity test assuming a 50% uncertainty in the rate coefficients of aqueous-phase reactions that we previously assumed had a 20% uncertainty in Figure 7. The resulting concentration uncertainty slightly changed for sulfate but almost doubled for hydrogen peroxide in the cloud case (Figure 8). The effects were small on ozone, PAN, formaldehyde, methylperoxide, and acetaldehyde. We also conducted a sensitivity test assuming a 100% uncertainty in the photolysis rates. We found that increasing the uncertainty in photolysis reactions increases concentration uncertainties for ozone, hydrogen peroxide, and aldehydes but has small effects on those for sulfate and PAN.

The above results may have important implications for model evaluation and chemical mechanism compression. Several studies have shown that observed concentrations may be captured by three-dimensional (3-D) chemical transport models to some extent, but disagreements between predictions and observations persist for species of photochemical origin such as H_2O_2 [*Horowitz et al.*, 1998] and PAN [*Liang et al.*, 1998]. Such disagreements may partly originate from the uncertainty in chem-

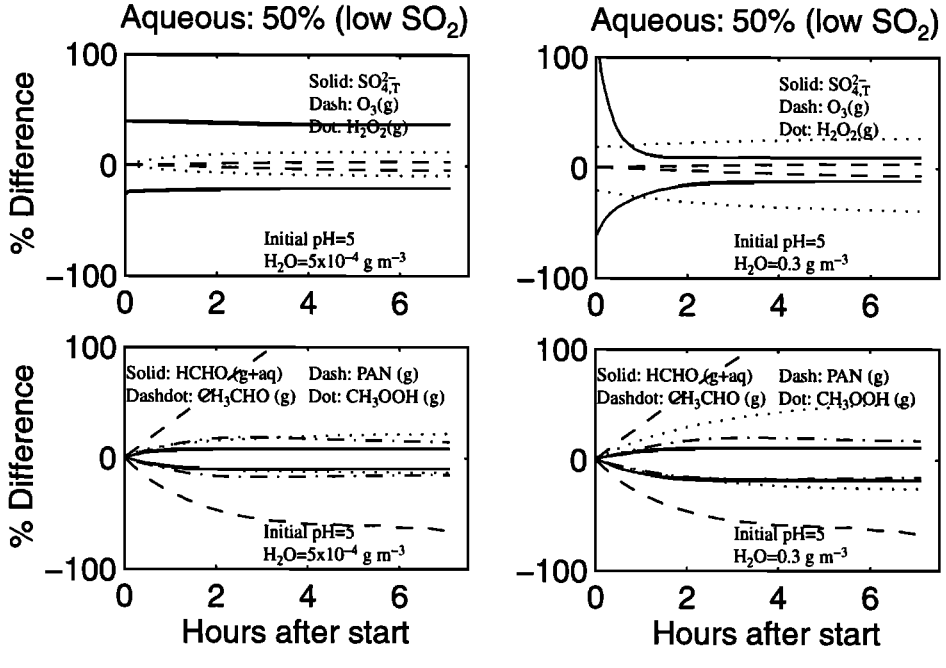

Figure 8b. Same as Figure 7b, except that the uncertainty of aqueous-phase reaction rate coefficients are assumed to be 50%, instead of 20% in Figure 7b.

Table 3. A Compressed Chemical Mechanism for the Oxidation of Sulfur Dioxide

	Reaction	Rate constant	k_1	k_2	Reference
		Gas Phase			
1	$O_3+h\nu \rightarrow O(^1D)+O_2$	a			
	$O_3+h\nu \rightarrow O+O_2$	a			
2	$O(^1D)+N_2 \rightarrow O+N_2$	b	1.8×10^{-11}	-107	
3	$O(^1D)+O_2 \rightarrow O+O_2$	b	3.2×10^{-11}	-67	
4	$O(^1D)+H_2O \rightarrow OH+OH$	2.2×10^{-10}			
5	$O+O_2+M \rightarrow O_3+M$	c	5.7×10^{-34}	2.8	
		$k_3=1$, $k_4=0$	$k_5=0$, $k_6=1$.	$k_7=0$, $k_8=0$	
6	$NO_2+h\nu \rightarrow NO+O$	a			
7	$O_3+NO \rightarrow NO_2+O_2$	b	1.8×10^{-12}	1370	
8	$O_3+OH \rightarrow HO_2+O_2$	b	1.9×10^{-12}	1000	
9	$O_3+HO_2 \rightarrow OH+O_2+O_2$	b	1.4×10^{-14}	600	
10	$O_3+NO_2 \rightarrow O_2+NO_3$	b	1.2×10^{-13}	2450	
11	$H_2O_2+h\nu \rightarrow OH+OH$	a			
12	$H+O_2+M \rightarrow HO_2+M$	c	4.3×10^{-32}	1.8	
		$k_3=7.5\times10^{-11}$, $k_4=0$	$k_5=-0.5978$, $k_6=1$	$k_7=0$, $k_8=0$	
13	$OH+HO_2 \rightarrow H_2O+O_2$	b	4.8×10^{-11}	-250	
14	$HO_2+NO \rightarrow OH+NO_2$	b	3.7×10^{-12}	-240	
15	$HO_2+HO_2 \rightarrow H_2O_2$	b	2.2×10^{-13}	-600	
	$HO_2+HO_2+M \rightarrow H_2O_2$	d	1.5×10^{-14}	-980	
16	$HO_2+HO_2+H_2O \rightarrow H_2O_2$	b	3.1×10^{-34}	-2800	
	$HO_2+HO_2+H_2O+M \rightarrow H_2O_2$	d	2.1×10^{-35}	-3180	
17	$OH+H_2 \rightarrow H_2O+H$	b	7.7×10^{-12}	2100	
18	$CO+OH \rightarrow H+CO_2$	e	1.3×10^{-13}	0.6	
19	$OH+CH_4 \rightarrow CH_3O_2+H_2O$	b	2.3×10^{-12}	1765	
20	$CH_3O_2+NO \rightarrow CH_2O+HO_2+NO_2$	b	4.2×10^{-12}	-180	
21	$CH_3O_2+HO_2 \rightarrow CH_3OOH+O_2$	b	3.8×10^{-13}	-780	
22	$CH_3O_2+CH_3O_2 \rightarrow CH_3OH+CH_2O$	f1	1.1×10^{-13}	-365	
		$k_3=5.94\times10^{-13}$, $k_4=505$			
23	$CH_3O_2+CH_3O_2 \rightarrow 2\ CH_2O+2\ HO_2$	b	5.9×10^{-13}	505	
24	$CH_3OOH+h\nu \rightarrow CH_2O+H+OH$	a			
25	$CH_3OOH+OH \rightarrow CH_3O_2+H_2O$	b	1.9×10^{-12}	-190	
	$CH_3OOH+OH \rightarrow CH_2O+OH+H_2O$	b	$1\ 0\times10^{-12}$	-190	
26	$CH_2O+OH \rightarrow CO+HO_2+H_2O$	b	8.6×10^{-12}	-20	
27	$CH_2O+h\nu \rightarrow H+H+CO$	a			
28	$CH_2O+h\nu \rightarrow H_2+CO$	a			
29	$NO_2+OH+M \rightarrow HNO_3+M$	c	2.0×10^{-30}	2.9	
		$k_3=6.7\times10^{-11}$, $k_4=0.6$	$k_5=-0.844$, $k_6=1$	$k_7=0$, $k_8=0$	
30	$HNO_3+h\nu \rightarrow OH+NO_2$	a			
31	$HNO_3+OH \rightarrow H_2O+NO_3$	f2	7.2×10^{-15}	785	
		$k_3=4.1\times10^{-16}$, $k_4=1440$	$k_5=1\ 9\times10^{-33}$, $k_6=725$		
32	$NO+OH+M \rightarrow HNO_2+M$	c	5.8×10^{-31}	2 4	
		$k_3=4.5\times10^{-11}$, $k_4=0$	$k_5=-0.1054$, $k_6=1$	$k_7=0$, $k_8=0$	
33	$HNO_2+h\nu \rightarrow OH+NO$	a			
34	$HNO_2+OH \rightarrow H_2O+NO_2$	b	2.7×10^{-12}	-260	
35	$HO_2+NO_2+M \rightarrow HNO_4+M$	c	1.4×10^{-31}	3.2	
		$k_3=4.7\times10^{-12}$, $k_4=0$	$k_5=-0.5108$, $k_6=1$	$k_7=0$, $k_8=0$	
36	$HNO_4+M \rightarrow HO_2+NO_2+M$	c	4.0×10^{-6}	0	
		$k_3=2.6\times10^{15}$, $k_4=0$	$k_5=-0.5108$, $k_6=1$	$k_7=10000$, $k_8=10900$	
37	$HNO_4+h\nu \rightarrow OH+NO_3$	a			
	$HNO_4+h\nu \rightarrow HO_2+NO_2$	a			
38	$HNO_4+OH \rightarrow 0.5\ NO_2+0.5\ H_2O_2+0.5\ NO_3$	b	1.5×10^{-12}	-360	
39	$NO_3+h\nu \rightarrow NO_2+O$	a			
	$NO_3+h\nu \rightarrow NO+O_2$	a			
40	$NO_3+NO \rightarrow 2\ NO_2$	b	$1\ 8\times10^{-11}$	-110	
41	$NO_3+HCHO \rightarrow HNO_3+HO_2+CO$	5.8×10^{-16}			
42	$NO_2+NO_3+M \rightarrow N_2O_5+M$	c	2.1×10^{-30}	3.4	
		$k_3=2\times10^{-12}$, $k_4=-0.2$	$k_5=-1.11$, $k_6=1$	$k_7=0$, $k_8=0$	
43	$N_2O_5+M \rightarrow NO_2+NO_3+M$	c	7.9×10^{-4}	3.5	
		$k_3=9.7\times10^{14}$, $k_4=-0.1$	$k_5=-1.11$, $k_6=1$	$k_7=11000$, $k_8=11080$	
44	$N_2O_5+h\nu \rightarrow NO_3+NO_2$	a			
	$N_2O_5+h\nu \rightarrow NO_3+NO+O$	a			
45	$SO_2+OH \rightarrow H_2SO_4+HO_2$	c	4.0×10^{-31}	3.3	
		$k_3=2.0\times10^{-12}$, $k_4=0$	$k_5=-0.8$, $k_6=1$	$k_7=0$, $k_8=0$	
46	$SO_2+O \rightarrow H_2SO_4+M$	b	3.2×10^{-32}	1000	
1'	$CH_3CHO+h\nu \rightarrow CH_3O_2+HO_2+CO$	a			
	$CH_3CHO+h\nu \rightarrow CH_4+CO$	a			
2'	$C_2H_5OOH+h\nu \rightarrow OH+HO_2+CH_3CHO$	a			
3'	$CH_3CHO+OH \rightarrow CH_3CO_3+H_2O$	b	5.6×10^{-12}	-310	
4'	$CH_3CO_3+NO_2+M \rightarrow CH_3C(O)O_2NO_2+M$	c	2.1×10^{-28}	7.1	
		$k_3=1.2\times10^{-11}$, $k_4=0.9$	$k_5=-1.2$, $k_6=1$	$k_7=0$, $k_8=0$	
5'	$CH_3C(O)O_2NO_2 \rightarrow CH_3CO_3+NO_2$	c	3.9×10^{-3}	0	
		$k_3=5.4\times10^{16}$, $k_4=0$	$k_5=-1.2$, $k_6=1$	$k_7=12100$, $k_8=13830$	

Table 3. (continued)

	Reaction	Rate constant	k_1	k_2	Reference
6'	$OH+CH_3C(O)O_2NO_2 \rightarrow CH_3CO_3+HNO_3$	b	9.5×10^{-13}	-650	
7'	$CH_3CO_3+NO \rightarrow CH_3O_2+NO_2+CO_2$	2.0×10^{-11}			
8'	$C_2H_6+OH \rightarrow C_2H_5O_2+H_2O$	b	7.9×10^{-12}	1030	
9'	$C_2H_5O_2+NO \rightarrow CH_3CHO+NO_2+HO_2$	8.7×10^{-12}			
10'	$C_2H_5OH+OH \rightarrow HO_2+CH_3CHO$	b	4.1×10^{-12}	70	
11'	$C_2H_5O_2+HO_2 \rightarrow C_2H_5OOH+O_2$	b	2.7×10^{-13}	-1000	
12'	$HO_2+CH_3CO_3 \rightarrow CH_3COOH+O_3$	b	3.0×10^{-13}	-1040	
	$HO_2+CH_3CO_3 \rightarrow CH_3C(O)OOH$	b	1.3×10^{-13}	-1040	
13'	$CH_3CO_3+CH_3CO_3 \rightarrow 2CH_3O_2$	b	2.8×10^{-12}	-530	
14'	$CH_3CO_3+CH_3O_2 \rightarrow HCHO+CH_3O_2+HO_2$	b	4.4×10^{-12}	-272	
	$CH_3CO_3+CH_3O_2 \rightarrow CH_3COOH+HCHO$	b	7.2×10^{-13}	-272	
		Gas-Aqueous Interaction			
1	$N_2O_5 \rightarrow 2\ HNO_3$	g	108	0	
2	$O_3 \rightarrow O_3(aq)$	g	48	0.1	
3	$O_3(aq) \rightarrow O_3$	h	1.1×10^{-2}	-4.76	HC85
4	$HO_2 \rightarrow HO_2(aq)$	g	33	0.1	
5	$HO_2(aq) \rightarrow HO_2$	h	$2.0(\pm1)\times10^{3}$	-13.2	Sc84
6	$OH \rightarrow OH(aq)$	g	17	0.1	
7	$OH(aq) \rightarrow OH$	h	20	-10.5	KSH85
8	$H_2O_2 \rightarrow H_2O_2(aq)$	g	34	0.1	
9	$H_2O_2(aq) \rightarrow H_2O_2$	h	$1.1(\pm0.36)\times10^{5}$	-13.2	MD81,YO84,LK86
10	$HCOOH \rightarrow HCOOH(aq)$	g	46	0.1	
11	$HCOOH(aq) \rightarrow HCOOH$	h	$5.6(\pm2)\times10^{3}$	-11.4	Be92
12	$CH_3OOH \rightarrow CH_3OOH(aq)$	g	48	0.1	
13	$CH_3OOH(aq) \rightarrow CH_3OOH$	h	220	-11.2	LK86
14	$SO_2 \rightarrow SO_2(aq)$	g	64	0.1	
15	$SO_2(aq) \rightarrow SO_2$	h	1.2(±0.03)	-6.27	OH89
16	$CH_3O_2 \rightarrow CH_3O_2(aq)$	g	47	0.1	
17	$CH_3O_2(aq) \rightarrow CH_3O_2$	h	5.9	-11.2	Jb86
		Aqueous Phase			
1	$OH(aq)+HO_2(aq) \rightarrow H_2O(aq)+O_2(aq)$	i	$6.6(\pm0.55)\times10^{9}$	3	SRF68,Th63
2	$OH(aq)+O_2^- \rightarrow OH^-+O_2(aq)$	i	$0.85(\pm0.15)\times10^{10}$	3	BGHR88
3	$HO_2(aq)+O_2^- \rightarrow H_2O_2(aq)+O_2(aq)+OH^-$	i	$0.97(\pm0.06)\times10^{8}$	2.1	BCAR85
4	$HO_2(aq)+HO_2(aq) \rightarrow H_2O_2(aq)+O_2(aq)$	i	$8.3(\pm0.7)\times10^{5}$	5.4(±0.5)	BCAR85
5	$OH(aq)+H_2O_2(aq) \rightarrow HO_2(aq)+H_2O(aq)$	i	2.7×10^{7}	3.4	CSC82,BGHR88
6	$O_2^-+O_3(aq) \rightarrow OH(aq)+OH^-+2\ O_2(aq)$	i	$1.5(\pm0.05)\times10^{9}$	3	SHH83,BCAR85
7	$H_2O_2(aq)+hv \rightarrow OH(aq)+OH(aq)$	a	Radiation	dependent	GW81
8	$OH(aq)+HSO_3^- \rightarrow SO_3^-+H_2O(aq)$	i	4.5×10^{9}	3	HN87
9	$HSO_3^-+H^++H_2O_2(aq) \rightarrow SO_4^{2-}+2\ H^+$	j	$7.5(\pm1.5)\times10^{7}$	9.45(±0.05)	HC85
10	$H_2C(OH)_2+OH(aq) \rightarrow HO_2(aq)+HCOOH(aq)$	i	$7.7(x3.8)\times10^{8}$	2(1±.34)	CW94
11	$OH(aq)+SO_3^{2-} \rightarrow SO_3^-+OH^-$	i	$5.5(\pm0.35)\times10^{9}$	3	HN87,AB64,BGHR88
12	$HCOO^-+OH(aq) \rightarrow CO_2+HO_2(aq)+OH^-$	i	$3.2(x3.8)\times10^{9}$	2.5(1±.51)	CW94
13	$HSO_3^-+H^++CH_3OOH(aq) \rightarrow SO_4^{2-}+2\ H^++CH_3OH(aq)$	k	1.9×10^{7}	7.56	HC85
14	$SO_3^{2-}+SO_4^- \rightarrow SO_4^{2-}+SO_3^-$	i	7.5×10^{8}	3	WTTWD89
15	$HSO_3^-+SO_4^- \rightarrow SO_4^{2-}+SO_3^-+H^+$	i	$7.5(\pm0.6)\times10^{8}$	3	WTTWD89
16	$HSO_3^-+H_2C(OH)_2 \rightarrow HOCH_2SO_3^-$	i	0.43(±0.02)	6(±0.2)	BH84
17	$SO_3^{2-}+H_2C(OH)_2 \rightarrow HOCH_2SO_3^-+OH^-$	i	$1.4(\pm0.03)\times10^{4}$	4.9(±0.1)	BH84
18	$HSO_3^-+O_3(aq) \rightarrow SO_4^{2-}+H^+$	i	3.7×10^{5}	11.06	HC85
19	$SO_3^{2-}+O_3(aq) \rightarrow SO_4^{2-}$	i	1.5×10^{9}	10.56	HC85
20	$SO_4^-+OH^- \rightarrow SO_4^{2-}+OH(aq)$	i	8.0×10^{7}	3	MN78
21	$SO_4^-+H_2O_2(aq) \rightarrow H^++SO_4^{2-}+HO_2(aq)$	i	$1.2(\pm0.1)\times10^{7}$	4	WTTWD89
22	$SO_4^-(+H_2O(aq)) \rightarrow SO_4^{2-}+H^++OH(aq)$	l	440(±50)	3.7(±0.1)	BB96
23	$SO_4^-+HCOO^- \rightarrow SO_4^{2-}+CO_2(aq)+HO_2(aq)$	i	$1.1(\pm0.05)\times10^{8}$	3	WTTWD89
24	$CH_3O_2(aq)+O_2^- \rightarrow CH_3OOH(aq)+OH^-+O_2(aq)$	i	5.0×10^{7}	2.1	Jb86
25	$HCOOH(aq)+OH(aq) \rightarrow H_2O(aq)+CO_2(aq)+HO_2(aq)$	i	$1.1(x3.9)\times10^{8}$	2(1±0.41)	CW94
26	$O_3(aq)+H_2O_2(aq)+OH^- \rightarrow OH(aq)+O_2^-+O_2(aq)+H_2O(aq)$	k	4.4×10^{8}	-8	SH82
27	$HOCH_2SO_3^-+OH^- \rightarrow SO_3^{2-}+H_2C(OH)_2$	i	$3.7(\pm1)\times10^{3}$	9	DNHW86,MTH86
28	$CH_3OOH(aq)+OH(aq) \rightarrow H_2C(OH)_2+OH(aq)$	i	1.9×10^{7}	3.7	Jb86
	$CH_3OOH(aq)+OH(aq) \rightarrow CH_3O_2(aq)+H_2O$	i	2.7×10^{7}	3.4	Jb86
29	$HOCH_2SO_3^-+OH(aq) \rightarrow H_2C(OH)_2+SO_3^-+H^++OH^-$	i	1.3×10^{9}	3	MEFH89
30	$SO_4^-+HO_2(aq) \rightarrow SO_4^{2-}+H^++O_2(aq)$	i	5.0×10^{9}	3	Jb86
31	$SO_4^-+O_2^- \rightarrow SO_4^{2-}+O_2(aq)$	i	5.0×10^{9}	3	Jb86
32	$HCOO^-+O_3(aq) \rightarrow CO_2(aq)+OH(aq)+O_2^-$	i	1.0×10^{2}	11	HB83
33	$SO_3^-+HCOO^- \rightarrow HSO_3^-+CO_2(aq)+O_2^-$	i	1.4×10^{4}	8	Jb86
34	$SO_4^-+NO_2^- \rightarrow SO_4^{2-}+NO_2(aq)$	i	9.8×10^{8}	3.0	WTTWD89
35	$SO_3^-+HSO_3^- \rightarrow HSO_5^-+SO_3^-$	i	2.5×10^{4}	7.7	HN87
36	$HSO_5^-+OH(aq) \rightarrow SO_5^-+H_2O(aq)$	i	1.7×10^{7}	3.8	MN77
37	$HSO_5^-+HSO_3^-+H^+ \rightarrow 2\ SO_4^{2-}+3\ H^+$	k	$1.7(\pm1)\times10^{7}$	4(±2.2)	Mc87,BH88a
38	$SO_5^-+HSO_3^- \rightarrow SO_4^-+SO_4^{2-}+H^+$	i	7.5×10^{4}	7.0	HN87
39	$O_2^-+SO_5^- \rightarrow O_2(aq)+HSO_5^-+OH^-$	i	1.0×10^{8}	2.1	Jb86
40	$NO_2^-+OH(aq) \rightarrow NO_2(aq)+OH^-$	i	1.0×10^{10}	3.0	Tr70

Table 3. (continued)

	Reaction	Rate constant	k_1	k_2	Reference
41	$H_2O(aq) <-> OH^- + H^+$	m	1.0×10^{-14}	13.34	HC85
42	$HO_2(aq) <-> O_2^- + H^+$	n	1.6×10^{-5}		BCAR85
43	$HCOOH(aq) <-> HCOO^- + H^+$	n	1.8×10^{-4}	0.3	SM64
44	$HNO_2(aq) <-> NO_2^- + H^+$	n	5.1×10^{-4}	2.5	SW81
45	$SO_2(aq) <-> HSO_3^- + H^+$	n	1.5×10^{-2}	-4	OH89
46	$HSO_3^- <-> SO_3^{2-} + H^+$	n	6.3×10^{-8}	-2.99	OH89
47	$HSO_4^- <-> SO_4^{2-} + H^+$	n	0.01	-5.44	SM76
1'	$CH_3COOH(aq) + OH(aq) -> HO_2(aq) + H_2C(OH)_2$	i	$1.8(\times4.1)\times10^{7}$	$2.6(1\pm0.26)$	CW94
2'	$CH_3COO^- + OH(aq) -> O_2^- + H_2C(OH)_2$	i	$7.5(\times3.8)\times10^{7}$	$3.5(1\pm0.23)$	CW94
3'	$CH_3COOH <-> CH_3COOH(aq)$	o	8.8×10^{3}	-12.8	KG86
4'	$CH_3COOH(aq) <-> CH_3COO^- + H^+$	n	1.7×10^{-5}	-0.1	MS77
5'	$HCHO <-> H_2C(OH)_2$	o	3.0×10^{3}	-14.3	BH88b
6'	$HNO_2 <-> HNO_2(aq)$	o	49	-9.5	SW81
1"	$Cl^- + OH(aq) + H^+ -> Cl(aq)$	i	$1.4(\pm0.1)\times10^{10}$		JPS73,WYS97
2"	$Cl_2^- + HO_2(aq) -> 2\,Cl^- + H^+ + O_2(aq)$	i	$4.2(\pm0.3)\times10^{9}$		RN79,WYS97
3"	$Cl_2^- + O_2^- -> 2\,Cl^- + O_2(aq)$	i	1.0×10^{9}		RN79
4"	$Cl_2^- + H_2O_2(aq) -> 2\,Cl^- + H^+ + HO_2(aq)$	i	1.4×10^{5}		HN78
5"	$H_2O_2(aq) + Cl(aq) -> Cl^- + HO_2(aq) + H^+$	i	4.5×10^{7}		Jn97
6"	$NO_3(aq) + Cl^- -> NO_3^- + Cl(aq)$	i	$1.0(\pm0.2)\times10^{7}$	$8.6(\pm1)$	EHZ92
7"	$Cl(aq) -> Cl^- + H^+ + OH(aq)$	l	1.0×10^{5}		WTTWD89
8"	$SO_4^- + Cl^- -> SO_4^{2-} + Cl(aq)$	i	2.0×10^{8}		WTTWD89
9"	$CH_3OH(aq) + Cl_2^- -> 2\,Cl^- + H_2C(OH)_2 + H^+ + HO_2(aq)$	i	3.5×10^{3}		HN78
10"	$HCOOH(aq) + Cl_2^- -> 2\,Cl^- + CO_2(aq) + H^+ + HO_2(aq)$	i	$5(\pm1)\times10^{3}$		HN78,WYS97
11"	$HCOO^- + Cl_2^- -> 2\,Cl^- + CO_2(aq) + HO_2(aq)$	i	$1.6(\pm0.2)\times10^{6}$		HN78,WYS97
12"	$Cl_2^- + OH^- -> 2\,Cl^- + OH(aq)$	i	4.0×10^{6}	4.3	JHZ97
13"	$Cl_2^- + HSO_3^- -> 2\,Cl^- + SO_3^- + H^+$	i	3.4×10^{8}	3	HN87,Jn97
14"	$Cl_2^- + SO_3^{2-} -> 2\,Cl^- + SO_3^-$	i	1.6×10^{8}	3	HN87,Jn97
15"	$NO_2^- + Cl_2^- -> NO_2(aq) + 2\,Cl^-$	i	$2.3(\pm0.2)\times10^{8}$		HN78,WYS97
16"	$Cl_2^- <-> Cl(aq) + Cl^-$	l	5.3×10^{-6}		Jn99
17"	$Cl(aq) + h\nu -> Cl^- + H^+ + OH(aq)$	a	Radiation	dependent	Jn99
18"	$Cl_2^- + h\nu -> 2\,Cl^- + H^+ + OH(aq)$	a	Radiation	dependent	Jn99

Rate constant parameters are taken from *Atkinson et al.* [1997] for gas-phase reactions. The sources for gas-aqueous interactions and aqueous-phase reactions are indicated. Equilibrium equations are denoted with <->. The calculation of activity coefficients is described in the text. Reactions related to chlorine radical in aqueous phase (1"-17") were not chosen in the compressed simulation and are listed here for informational purposes AB64, *Adams and Boag* [1964]; BB96, *Bao and Barker* [1996]; BCAR85, *Bielski et al.* [1985]; Be92, *Betterton* [1992]; BGHR88, *Buxton et al.* [1988]; BH84, *Boyce and Hoffmann* [1984]; BH88a, *Betterton and Hoffmann* [1988a]; BH88b, *Betterton and Hoffmann* [1988b]; CSC82, *Christensen et al.* [1982]; CW94, *Chin and Wine* [1994]; DNHW86, *Deister et al* [1986]; EHZ92, *Exner et al.* [1992]; GW81, *Graedel and Weschler* [1981]; HB83, *Hoigne and Bader* [1983]; HC85, *Hoffmann and Calvert* [1985]; HN78, *Hagesawa and Neta* [1978]; HN87, *Huie and Neta* [1987]; Jb86, *Jacob* [1986]; Jn97, *Jacobson* [1997a]; Jn99, *Jacobson* [1999]; JHZ97, *Jacobi et al.* [1997]; JPS73, *Jayson et al.* [1973]; KG86, *Keene and Galloway* [1986]; KSH85, *Klaning et al.* [1985]; LK86, *Lind and Kok* [1986]; Mc87, *McElroy* [1987]; MD81, *Martin and Damschen* [1981]; MEFH89, *Martin et al.* [1989]; MN77, *Maruthamuthu and Neta* [1977]; MN78, *Maruthamuthu and Neta* [1978]; MS77, *Martell and Smith* [1977]; MTH86, *Munger et al.* [1986]; OH89, *Olson and Hoffmann* [1989]; RN79, *Ross and Neta* [1979]; Sc84, *Schwartz* [1984]; SH82, *Staehelin and Hoigne* [1982]; SHH83, *Sehested et al.* [1983]; SM64, *Sillen and Martell* [1964]; SM76, *Smith and Martell* [1976]; SRF68, *Sehested et al.* [1968]; SW81, *Schwartz and White* [1981]; Th63, *Thomas* [1963]; Tr70, *Treinin* [1970]; WTTWD89, *Wine et al.* [1989]; WYS97, *Walcek et al.* [1997]; YO84, *Yoshizumi et al.* [1984]. (±X) denotes that k may increment by X or -X, (1±X) that k may vary by a factor of (1+X) or (1-X), and (xF) that k may vary by F times or 1/F times. The significance is at 1σ level, and for precision only.

[a] Photodissociation reaction. Cross sections and quantum yields are taken from *Atkinson et al.* [1997]. Actinic fluxes are calculated as described in section 2.

[b] Rate constant $k = k_1 \exp(-k_2/T)$. The unit is s^{-1} for first-order reactions, $molecule^{-1}cm^3s^{-1}$ for second-order reactions, and $molecule^{-2}cm^6s^{-1}$ for third-order reactions. T is temperature in Kelvin.

[c] Rate constant $k = AB/(A+B)\,\exp\{k_5[1+((\log_{10}(A/B))/k_6)^2]^{-1}\}$, where $A = k_1[M](300/T)^{k_2}\exp(-k_7/T)$, $B = k_3(300/T)^{k_4}\exp(-k_8/T)$, and [M] denotes the number density of air molecules in molecules cm^{-3}.

[d] Rate constant $k = 1\times10^{-19}[M]k_1\exp(-k_2/T)$, and [M] is as in footnote c.

[e] Rate constant $k = k_1(1+k_2P)$, where P is pressure in atmosphere.

[f1] Rate constant $k = k_1\exp(-k_2/T) - k_3\exp(-k_4/T)$.

[f2] Rate constant $k = k_1\exp(k_2/T) + R_2R_3/(R_2+R_3)$ where $R_2 = k_3\exp(k_4/T)$, $R_3 = k_5[M]\exp(k_6/T)$, and [M] is as in footnote c.

[g] Rate constant $k = 3\,D_g\,L/(\Lambda\,r^2)$. $D_g = 9.45\times10^{17}/[M]\,\sqrt{T}\,(0.03472+1/k_1)$. L is the volume mixing ratio of liquid water. $\Lambda = 1 + (\lambda+1.3(1/k_2-1))$, and $\lambda = (0.71+1.3\beta)/(1+\beta)$. $\beta = 4.54\times10^{-15}\sqrt{V_g^2+V_{air}^2}$. $V_g = \sqrt{8\,R\,T/(\pi\,k_1)}$, *and* $V_{air} = \sqrt{8\,R\,T/(28.8\pi)}$. $R = 8.31\times10^7$ is the ideal gas constant multiplied by a factor to keep Vs in the unit of cm s^{-1}. r is the radius of an aerosol droplet in cm.

[h] Rate constant $k = k_{n-1}/(0.082\,T\,L\,C)$ $C = k_1\exp(-500k_2(1/T - 1/298))$. k_{n-1} is the rate constant of its reverse reaction. L is as in g.

[i] Rate constant $k = C/D^2$. C is as in h. $D = 6.023\times10^{20}L$, and L is as in g.

[j] Rate constant $k = C/(D^2+13D[H^+])$. C and D are as in i, and $[H^+]$ is in the unit of the number of protons per cubic centimeter of air.

[k] Rate constant $k = C/D^2$. C and D are as in i.

[l] Rate constant k = C, and C is as in h

[m] Rate constant $k = C\,D^2$. C and D are as in i

[n] Rate constant k = C D. C and D are as in i.

[o] Rate constant k = C E. C is as in h. E = 0.082 T L, and L is as in g.

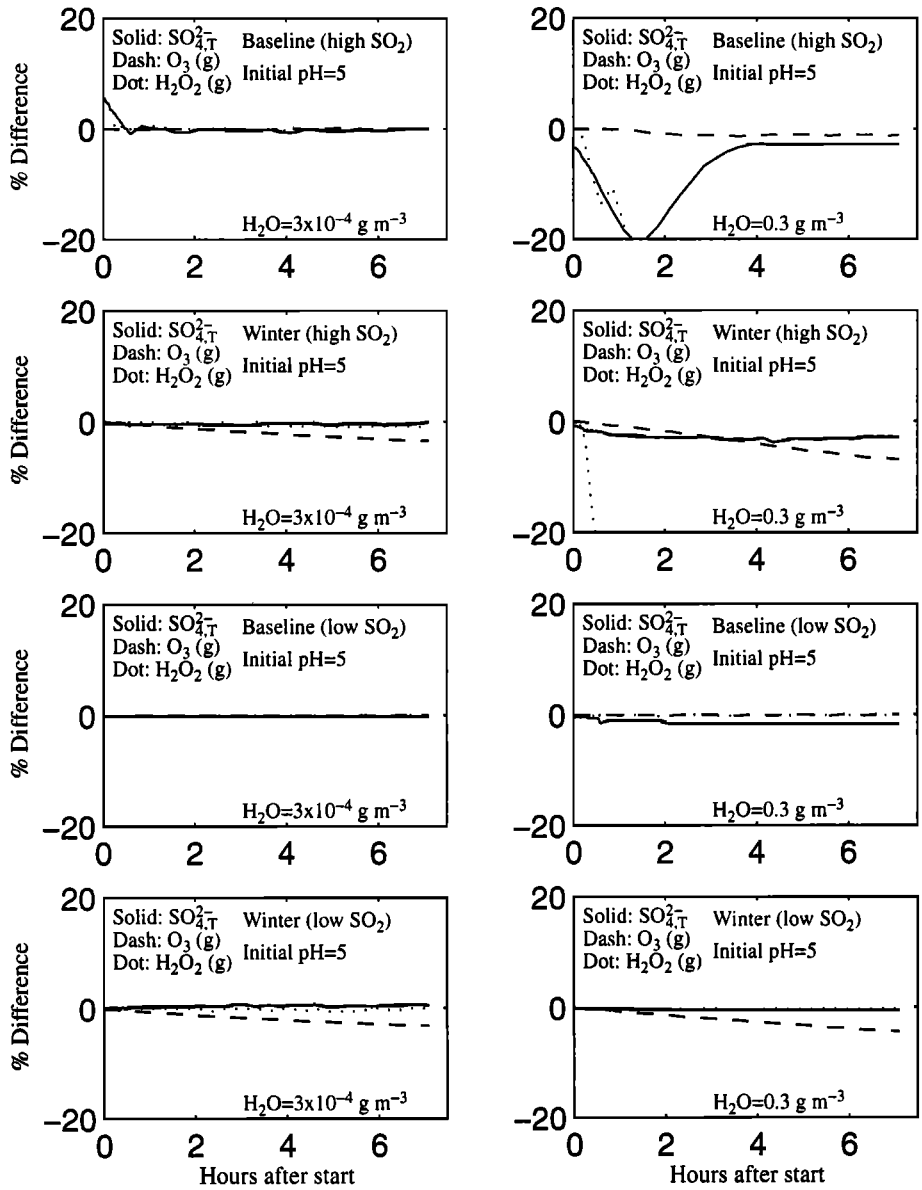

Figure 9. Percentage difference in concentrations of sulfate, ozone, and hydrogen peroxide between the simulations using the full mechanism and the simulations using the compressed mechanism.

ical rate coefficients. Since the uncertainty in chemical rate coefficients may propagate (~20% error to the calculated concentration of sulfate), the buildup of a compressed chemical mechanism with modest error criterion is warranted for photochemical production of sulfate.

5. Compressed Mechanism for Photochemical Oxidation of SO_2

The chemical mechanism for the CH_4-C_2H_6-CO-NO_x-SO_2 photochemical system contains several hundred reactions [*Atkinson et al.*, 1997] (see also section 2). In the original reaction list, there were many reactions peripheral to the production and loss of species important for SO_2 oxidation. A compressed reaction mechanism was developed by removing reactions accounting for less than 5% of the production and loss rates of species, in the pH range of 0 to 8 and the liquid water content range of 3×10^{-4} g m^{-3} to 9 g m^{-3} for all simulations listed in Table 2, except the compressed simulations. The remaining reactions forming the SO_2 oxidation mechanism are given in Table 3. The compressed reaction mechanism accounts for 95% of the chemical production and loss rates for the species important for SO_2 oxidation but contains just over 100 reactions. The method used for compressing the chemical mechanism has been used by authors in the combustion kinetics community [e.g., *Susnow et al.*, 1997]. Figure 9 shows the differences between the growth curves of sulfate, ozone, and hydrogen peroxide from the simulations using the full mechanism and those from the simulations using the compressed mechanism. It is shown that the differences are negligible in the noncloudy case. In the cloudy case the differences are a little larger, but within 10% for sulfate in most situations.

Figure 10 shows the percentage differences of the total sulfate produced between the simulations using the full mechanism and those using the compressed mechanism. It is shown that the differences are within 5% in the noncloudy case and within 10% in the cloudy case. When compounds containing more than one

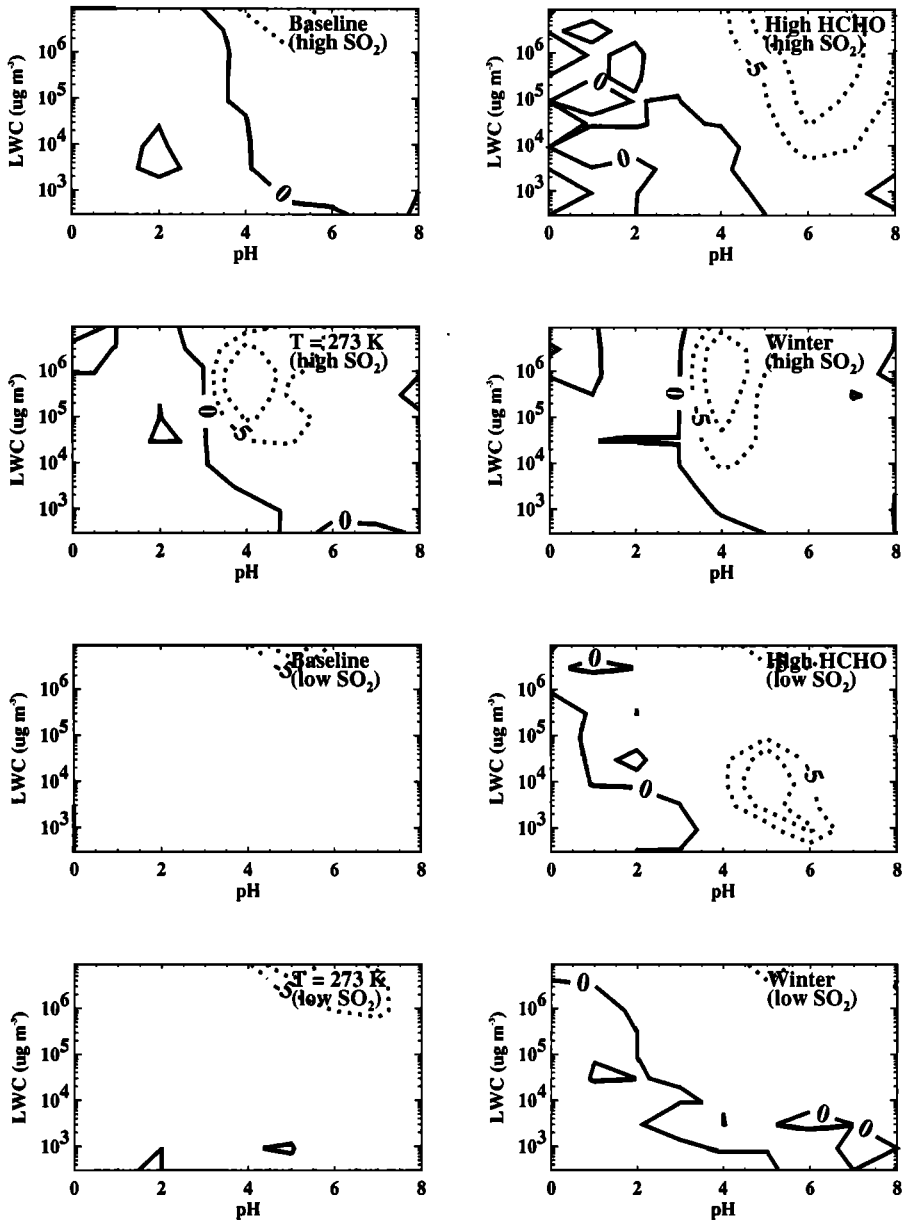

Figure 10. Percentage difference in the total sulfate produced between the simulations using the compressed mechanism and the simulations using the full mechanism over the (pH-liquid water content) plane.

carbon are neglected, the percentage differences of the total sulfate produced are typically 10% in the noncloudy case, as shown in Figure 11.

6. Conclusions

We examined factors controlling the photochemical oxidation of SO_2 in tropospheric aerosols using a gas-aqueous photochemical model. Over the pH range of 0 to 8 and the liquid water content range of 3×10^{-4} g m^{-3} to 9 g m^{-3}, we found that H_2O_2(aq) and O_3(aq) are the major oxidants for SO_2 in the aqueous phase when pH is held constant at below 5 and ≥6, respectively. When H_2O_2 is depleted from its reservoir, OH is an important oxidant for SO_2 in the aqueous phase when pH is held constant between 5 and 6. When pH is permitted to vary during the simulations, H_2O_2(aq) is the most important oxidant for SO_2 in the aqueous phase except at high liquid water content. In the latter case, OH(aq) is important when H_2O_2(aq) is depleted, and O_3(aq) is important when the final pH is above 4. We demonstrated that during the summer, aqueous-phase oxidation of SO_2 in aerosols is negligible compared with gas-phase oxidation of SO_2. When the temperature is low (273 K) and the relative humidity is high or the solar radiation is weak, the relative importance of aqueous-phase oxidation of SO_2 in aerosols is enhanced.

To facilitate global modeling of photochemical oxidation of SO_2, we constructed a compressed reaction mechanism for SO_2 oxidation. This mechanism accounts for over 95% of the production and loss rates of species important for SO_2 oxidation and contains a little more than 100 reactions. The resulting error from the use of this mechanism is within 5% for the production and

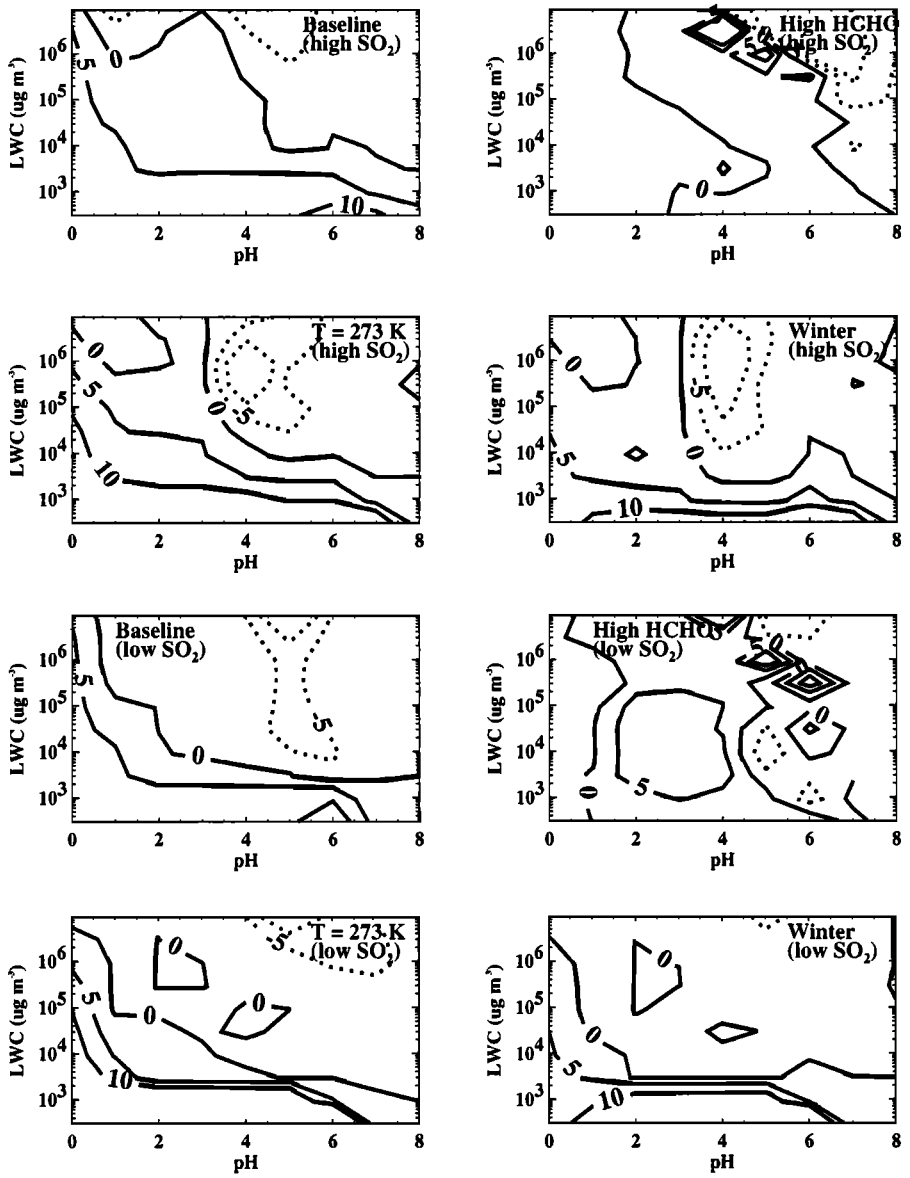

Figure 11. Percentage difference in the total sulfate produced between the simulations using the compressed mechanism excluding nonmethane hydrocarbons and the simulations using the full mechanism over the (pH-liquid water content) plane.

loss rates and within 10% for the concentrations of species determining SO_2 oxidation, significantly less than that propagated from uncertainties in chemical rate coefficients.

Appendix A: Calculation of Mean Mixed Activity Coefficients

Temperature-dependent mean binary activity coefficients γ_{12b} can be calculated from polynomials (A1)-(A3) from *Jacobson* [1999] for the 10 ion pairs of the NH_4^+-H^+-HSO_4^--SO_4^{2-}-NO_3^--HSO_3^--SO_3^{2-} system:

$$\ln\gamma_{12b}(T) = F_0 + F_1 m^{1/2} + F_2 m + F_3 m^{3/2} + \cdots \quad \text{(A1)}$$

where m is the molality of the ion pair 1-2 when it is the only solute in the solution with the ionic strength of I_m.

$$F_0 = B_0, \quad F_j = B_j + G_j T_L + H_j T_C, \quad j=1-5 \quad \text{(A2)}$$

and

$$T_L = T_0/T - 1, \quad T_C = 1 + \ln\left[\frac{T_0}{T}\right] - \frac{T_0}{T}, \quad T_0 = 298.15\ \text{K} \quad \text{(A3)}$$

Values of B, G, and H were listed by *Jacobson et al.* [1996] for most of the 10 electrolytes. Bisulfite and sulfite are assumed to behave as bisulfate and sulfate, respectively, and the data for the latter were also from Jacobson et al. [1996].

Temperature-dependent mean mixed activity coefficients (γ_{12m}) are estimated by Bromley's method that accounts for interactions of all ion pairs with opposite charges:

$$\log_{10}\gamma_{12m}(T) = -A_\gamma \frac{z_1 z_2 I_m^{1/2}}{1+I_m^{1/2}} + \frac{z_1 z_2}{z_1+z_2}\left[\frac{W_1}{z_1} + \frac{W_2}{z_2}\right] \quad \text{(A4)}$$

where A_γ is the Debye-Huckel parameter $(0.3915\ (T/298.15)^{1.5})$, z_1 and z_2 are the absolute value charges of cation 1 and anion 2, respectively. I_m is the total ionic strength of the mixture, and

$$W_1 = Y_{21}\left[\ln\gamma_{12b}(T) + A_\gamma\frac{z_1 z_2 I_m^{1/2}}{1+I_m^{1/2}}\right] + Y_{41}\left[\ln\gamma_{14b}(T) + A_\gamma\frac{z_1 z_4 I_m^{1/2}}{1+I_m^{1/2}}\right] + \cdots \quad \text{(A5)}$$

$$W_2 = X_{12}\left[\ln\gamma_{12b}(T) + A_\gamma\frac{z_1 z_2 I_m^{1/2}}{1+I_m^{1/2}}\right] + X_{32}\left[\ln\gamma_{32b}(T) + A_\gamma\frac{z_3 z_2 I_m^{1/2}}{1+I_m^{1/2}}\right] + \cdots \quad \text{(A6)}$$

and

$$Y_{21} = \left[\frac{z_1+z_2}{2}\right]^2\frac{m_{2,m}}{I_m},\quad X_{12} = \left[\frac{z_1+z_2}{2}\right]^2\frac{m_{1,m}}{I_m} \quad \text{(A7)}$$

X_{32}, X_{52}, etc., and Y_{41}, Y_{61}, etc., have similar expressions as X_{12} and Y_{21}. In equations (A1)-(A7), odd-numbered subscripts refer to cations and even-numbered subscripts refer to anions as appropriate.

Appendix B: Calculation of Activity Coefficients for Single Ions

In mixed electrolytes with the total ionic strength of I, the activity coefficient of a cation M (γ_M) is calculated from

$$\ln\gamma_M = z_M^2 F + \sum_a m_a(2B_{Ma} + Z\,C_{Ma}) + z_M\sum_c\sum_a m_c m_a C_{ca} \quad \text{(B1)}$$

The corresponding expression for a negative ion X is obtained by interchanging X for M, a for c, and c for a as appropriate.

In equation (B1), z denotes the charge of an individual ion, and $Z = \sum_i m_i|z_i|$. F, B, and C are defined as

$$F = f^\gamma + \sum_c\sum_a m_c m_a B'_{ca} \quad \text{(B2)}$$

$$f^\gamma = -A_\gamma[I^{1/2}/(1+bI^{1/2}) + (2/b)\ln(1+bI^{1/2})] \quad \text{(B3)}$$

$$B_{MX} = \beta^{(0)}_{MX} + \beta^{(1)}_{MX}\,g(\alpha_1 I^{1/2}) + \beta^{(2)}_{MX}\,g(\alpha_2 I^{1/2}) \quad \text{(B4)}$$

$$g(x) = 2[1 - (1+x)\exp(-x)]/x^2 \quad \text{(B5)}$$

$$B'_{MX} = [\beta^{(1)}_{MX}\,g'(\alpha_1 I^{1/2}) + \beta^{(2)}_{MX}\,g'(\alpha_2 I^{1/2})]/I \quad \text{(B6)}$$

$$g'(x) = -2[1 - (1 + x + x^2/2)\exp(-x)]/x^2 \quad \text{(B7)}$$

$$C_{MX} = C^\phi_{MX}/(2|z_M z_X|^{1/2}) \quad \text{(B8)}$$

where $\alpha_{1\text{-}2}$, $\beta^{(0\text{-}2)}_{MX}$, and C^ϕ_{MX} are parameters specific to ion pairs. Interactions of like charged ions are omitted from the original formula because they are insignificant [*Pitzer*, 1991, pp. 91-2].

References

Adams, G.E., and J.W. Boag, Spectroscopic studies of reactions of the OH radical, *Proc. Chem. Soc., 1*, 112-118, 1964.

Atkinson, R.A., D.L. Baulch, R.A. Cox, R.F. Hampson Jr., J.A. Kerr, M.J. Rossi, and J. Troe, Evaluated kinetic, photochemical, and heterogeneous data for atmospheric chemistry: Supplement V, IUPAC subcommittee on gas kinetic data evaluation for atmospheric chemistry, *J. Phys. Chem. Ref. Data, 26*, 521-1011, 1997.

Bao, Z.C., and J.R. Barker, Temperature and ionic strength effects on some reactions involving sulfate radical, *J. Phys. Chem., 100*, 9780-9787, 1996.

Betterton, E.A., Henry's law constants of soluble and moderately soluble organic gases: Effects on aqueous phase chemistry, in *Gaseous Pollutants: Characterization and Cycling*, edited by J.O. Nriagu, John Wiley, New York, 1992.

Betterton, E.A., and M.R. Hoffmann, Oxidation of aqueous SO_2 by peroxymonosulfate, *J. Phys. Chem., 92*, 5962-5965, 1988a.

Betterton, E.A., and M.R. Hoffmann, Henry's law constants of some environmentally important aldehydes, *Environ. Sci. Technol., 22*, 1415-1418, 1988b.

Bielski, B.H., D.E. Cabelli, R.L. Arudi, and A.B. Ross, Reactivity of HO_2/O_2^- radicals in aqueous solution, *J. Phys. Chem. Ref. Data, 14*, 1041-1100, 1985.

Boyce, S.C., and M.R. Hoffmann, Kinetics and mechanism of the formation of hydroxymethanesulfonic acid at low pH, *J. Phys. Chem., 88*, 4740-4746, 1984.

Bromley, L.A., Thermodynamic properties of strong electrolytes in aqueous solutions, *AIChE J., 19*, 313-320, 1973.

Buxton, G.V., C.L. Greenstock, W.P. Helman, and A.B. Ross, Critical review of rate constants for reactions of hydrated electrons, hydrogen atoms, and hydroxyl radicals (OH/O^-) in aqueous solutions, *J. Phys. Chem. Ref. Data, 17*, 513-886, 1988.

Chameides, W.L., and D.D. Davis, The free-radical chemistry of cloud droplets and its impact upon the composition of rain, *J. Geophys. Res., 87*, 4863-4877, 1982.

Chameides, W.L., and A.W. Stelson, Aqueous-phase chemical processes in deliquescent sea-salt aerosols: A mechanism that couples the atmospheric cycles of S and seasalt, *J. Geophys. Res., 98*, 9051-9054, 1993.

Chin, M., and P.H. Wine, A temperature dependent competitive kinetic study of the aqueous phase reactions of OH radicals with formate, formic acid, acetate, acetic acid, and hydrated formaldehyde, in *Environmental Aspects of Surface and Aquatic Photochemistry*, edited by G. Helz, R. Zepp, and D. Crosby, pp. 85-98, A.F. Lewis, New York, 1994.

Christensen, H., K. Sehested, and H. Corfitzen, Reactions of hydroxyl radicals with hydrogen peroxide at ambient and elevated temperatures, *J. Phys. Chem., 86*, 1588-1590, 1982.

Davies, C.W., The extent of dissociation of salts in water, VIII, An equation for the mean ionic activity coefficient of an electrolyte in water, and a revision of the dissociation constants of some sulphates, *J. Chem. Soc., 1*, 2093-2098, 1938.

Deister, U., R. Neeb, G. Helas, and P. Warneck, Temperature dependence of the equilibrium $H_2C(OH)_2(aq) + HSO_3^- = HOCH_2SO_3^- + H_2O$ in aqueous solution, *J. Phys. Chem., 90*, 3213-3217, 1986.

Exner, M., H. Herrmann, and R. Zellner, Laser-based studies of reactions of the nitrate radical in aqueous-solution, *Beri. Bunsen Ges. Phys. Chem., 96*, 470-477, 1992.

Exner, M., H. Herrmann, and R. Zellner, Rate constants for the reactions of the NO_3 radical with $HCOOH/HCOO^-$ and $CH3COOH/CH_3COO^-$ in aqueous solution between 278K and 328K, *J. Atmos. Chem., 18*, 359-378, 1994.

Finlayson-Pitts, B.J., and J.N. Pitts, *Atmospheric Chemistry: Fundamentals and Experimental Techniques*, John Wiley, New York, 1986.

Graedel, T.E., and C.J. Weschler, Chemistry within aqueous atmospheric aerosols and raindrops, *Rev. Geophys., 19*, 505-539, 1981.

Gurciullo, C.S., and S.N. Pandis, Effect of composition variations in cloud droplet populations on aqueous-phase chemistry, *J. Geophys. Res., 102*, 9375-9385, 1997.

Hagesawa, K., and P. Neta, Rate constants and mechanisms of reaction for Cl_2^- radicals, *J. Phys. Chem., 82*, 854-857, 1978.

Hoffman, M.R., and J.G. Calvert, Chemical transformation modules for Eulerian Acid Deposition Models, vol. 2, The aqueous-phase chemistry, *Report EPA/600/3-85/017*, U.S. Environ. Prot. Agency, Research Triangle Park, N.C., 1985.

Hoigne, J., and H. Bader, Rate constants of reactions of ozone with organic and inorganic compounds in water, 1, Non-dissociating organic compounds, *Water Res., 17*, 185-194, 1983.

Horowitz, L.W., J. Liang, G.M. Gardner, and D.J. Jacob, Export of reactive nitrogen from North America during summertime: Sensitivity of hydrocarbon chemistry, *J. Geophys. Res., 103*, 13,451-13,476, 1998.

Huie, R.E., and P. Neta, Rate constants for some oxidations of S(IV) by radicals in aqueous solutions, *Atmos. Environ., 21*, 1743-1747, 1987.

Jacob, D.J., Chemistry of OH in remote clouds and its role in the production of formic acid and peroxymonosulfate, *J. Geophys. Res., 91*, 9807-9826, 1986.

Jacobi, H.W., H. Herrmann, and R. Zellner, A laser flash-photolysis study of the decay of Cl-atoms and Cl_2^- radical-anions in aqueous solution at 298 K, *Ber. Bunsen Phys. Chem., 101*, 1909-1913, 1997.

Jacobson, M.Z., Development and application of a new air-pollution modeling system, II, Aerosol module structure and design, *Atmos. Environ., 31*, 131-144, 1997a.

Jacobson, M.Z., Development and application of a new air-pollution modeling system, III, Aerosol-phase simulations, *Atmos. Environ., 31*, 587-608, 1997b.

Jacobson, M.Z., *Fundamentals of Atmospheric Modeling*, Cambridge Univ. Press, New York, 1999.

Jacobson, M.Z., A. Tabazadeh, and R.P. Turco, Simulating equilibrium within aerosols and nonequilibrium between gases and aerosols, *J. Geophys. Res., 101*, 9079-9091, 1996.

Jayson, G.G., B.J. Parsons, and A.J. Swallow, Some simple, highly reactive, inorganic chlorine derivatives in aqueous solution, *Trans. Farad. Soc., 69*, 1597-1607, 1973.

Keene, W.C., and J.N. Galloway, Considerations regarding sources for formic and acetic acids in the troposphere, *J. Geophys. Res., 91*, 14,466-14,474, 1986.

Klaning, U.K., K. Sehested, and J. Holcman, Standard Gibbs free energy of formation of the hydroxyl radical in aqueous solution: Rate constants for the reaction $ClO_2^- + O_3 <-> O_3^- + ClO_2$, *J. Phys. Chem., 89*, 760-763, 1985.

Lelieveld, J., and P.J. Crutzen, Influence of cloud photochemical processes on tropospheric ozone, *Nature 343*, 227-233, 1990.

Liang, Jinyou, and D.J. Jacob, Effect of aqueous-phase cloud chemistry on tropospheric ozone, *J. Geophys. Res., 102*, 5993-6001, 1997.

Liang, Jinyou, L.W. Horowitz, D.J. Jacob, Y. Wang, A.M. Fiore, J.A. Logan, G.M. Gardner, and J.W. Munger, Seasonal budgets of reactive nitrogen species and ozone over the United States, and export fluxes to the global atmosphere, *J. Geophys. Res., 103*, 13,435-13,450, 1998.

Lind, J.A., and G.L. Kok, Henry's law determinations for aqueous solutions of hydrogen peroxide, methylhydroperoxide, and peroxyacetic acid, *J. Geophys. Res., 91*, 7889-7895, 1986.

Logan, J.A., M.J. Prather, S.C. Wofsy, and M.B. McElroy, Tropospheric chemistry: A global perspective, *J. Geophys. Res., 86*, 7210-7254, 1981.

Martell, A.E., and E.M. Smith, *Critical Stability Constants*, vol. 3, *Other Organic Ligands*, Plenum, New York, 1977.

Martin, L.R., and D.E. Damschen, Aqueous oxidation of sulfur dioxide by hydrogen peroxide at low pH, *Atmos. Environ., 15*, 1615, 1981.

Martin, L.R., M.P. Easton, J.W. Foster, and M.W. Hill, Oxidation of hydroxymethanesulfonic acid by Fenton reagent, *Atmos. Environ., 23*, 563-568, 1989.

Maruthamuthu, P., and P. Neta, Radiolytic chain decomposition of peroxomonophosphoric and peroxomonosulfuric acids, *J. Phys. Chem., 81*, 937-940, 1977.

Maruthamuthu, P., and P. Neta, Phosphate radicals, spectra, acid-base equilibria, and reactions with inorganic compounds, *J. Phys. Chem., 82*, 710-713, 1978.

McElroy, W.J., An experimental study of the reactions of some salts of oxy-sulphur acids and reduced sulphur compounds with strong oxidants (O_3, H_2O_2, and HSO_5^-), *Rep. TPRD/L/3141/R87*, Cent. Electr. Generating Board, Leatherhead, England, 1987.

Munger, J.W., C. Tiller, and M.R. Hoffmann, Identification of hydroxymethanesulfonate in fogwater, *Science, 231*, 247-249, 1986. Olson, T.M., and M.R. Hoffmann, Hydroxyalkylsulfonate formation: Its role as a S(IV) reservoir in atmospheric water droplets, *Atmos. Environ., 23*, 985-997, 1989.

Pandis, S.N., and J.H. Seinfeld, Sensitivity analysis of a chemical mechanism for aqueous-phase atmospheric chemistry, *J. Geophys. Res., 94*, 1105-1126, 1989.

Partanen, J.I., Determination of the molality scale dissociation-constants of formic, propionic and n-butyric acids in aqueous sodium-chloride solutions at 298.15 K, *Acta Chem. Scand., 50*, 492-498, 1996.

Pitzer, K.S., *Activity Coefficients in Electrolyte Solutions*, CRC Press, Boca Raton, Fla., 1991.

Press, W.H., S.A. Teukolsky, W.T. Vetterling, and B.P. Flannery, *Numerical Recipes in Fortran: The Art of Scientific Computing*, Cambridge Univ. Press, New York, 1992.

Rosenblatt, G.M., Estimation of activity coefficients in concentrated sulfite-sulfate solutions, *AIChE J., 27*, 619-626, 1981.

Ross, A.B., and P. Neta, Rate constants for reactions of inorganic radicals in aqueous solution, *Rep. NSRDS-NBS65*, U.S. Dept. of Commerce, Washington, D.C., 1979.

Schwartz, S.E., Gas- and aqueous-phase chemistry of HO_2 in liquid water clouds, *J. Geophys. Res., 89*, 11,589-11,598, 1984.

Schwartz, S.E., and W.H. White, Solubility equilibria of the nitrogen oxides and oxyacids in dilute aqueous solution, *Adv. Environ. Sci. Eng., 4*, 1, 1981.

Sehested, K., O.L. Rasmussen, and H. Fricke, Rate constants of OH with HO_2, O_2^-, and $H_2O_2^+$ from hydrogen peroxide formation in pulse-irradiated oxygenated water, *J. Phys. Chem., 72*, 626-631, 1968.

Sehested, K., J. Holcman, and E.J. Hart, Rate constants and products of the reactions of e_{aq}^-, O_2^-, and H with ozone in aqueous solutions, *J. Phys. Chem., 87*, 1951-1954, 1983.

Seinfeld, J.H., and S.N. Pandis, *Atmospheric Chemistry and Physics: From Air Pollution to Climate Change*, John Wiley, New York, 1998.

Sillen, G.L., and A.E. Martell, Stability constants of metal-ion complexes, *Spec. Publ. Chem. Soc., 17*, 357, 1964.

Smith, R.M., and A.E. Martell, *Critical Stability Constants*, vol. 4, *Inorganic Complexes*, Plenum, New York, 1976.

Staehelin, J., and J. Hoigne, Decomposition of ozone in water: Rate of initiation by hydroxide ions and hydrogen peroxide, *Environ. Sci. Technol., 16*, 676-681, 1982.

Susnow, R.G., A.M. Dean, W.H. Green, P. Peczak, and L.J. Broadbelt, Rate-based construction of kinetic models for complex systems, *J. Phys. Chem. A, 101*, 3731-3740, 1997.

Thomas, J.K., The rate constants for H atom reactions in aqueous solution, *J. Phys. Chem., 67*, 2593-2595, 1963.

Treinin, A., The photochemistry of oxyanions, *Isr. J. Chem., 8*, 103-113, 1970.

Walcek, C.J., H.H. Yuan, and W.R. Stockwell, The influence of aqueous-phase chemical reactions on ozone formation in polluted and nonpolluted clouds *Atmos. Environ., 31*, 1221-1237, 1997.

Wang, C., and J.S. Chang, A 3-dimensional numerical model of cloud dynamics, microphysics, and chemistry, 4, Cloud chemistry and precipitation chemistry, *J. Geophys. Res., 98*, 16,799-16,808, 1993.

Wine, P.H., Y. Tang, R.P. Thorn, J.R. Wells, and D.D. Davis, Kinetics of aqueous phase reactions of the SO_4^- radical with potential importance in cloud chemistry, *J. Geophys. Res., 94*, 1085-1094, 1989.

Yoshizumi, K., K. Aoki, I. Nouchi, T. Okita, T. Kobayashi, S. Kamakura, and M. Tajima, Measurements of the concentration of rainwater and of the Henry's law constant of hydrogen peroxide, *Atmos. Environ., 18*, 395-401, 1984.

M.Z. Jacobson and J. Liang, Department of Civil and Environmental Engineering, Stanford University, Terman Engineering Center, Room M-13, Stanford, CA 94305-4020. (jacobson@ce.stanford.edu; jinyouliang@yahoo.com)

(Received August 21, 1998; revised January 27, 1999; accepted February 3, 1999.)